

Answers to Referee#1

We thank the referee for his/her constructive remarks and suggestions. We answer below to the specific comments.

p. 24628, line 18-21. Can you please clarify in the text if ozone isotopologues were fitted in the retrieval of all stations or only Harestua? Or what is the difference in the fit of the Harestua. May be it is better to describe algorithm for all stations with the exception of Harestua and then describe algorithm for Harestua station separately.

Harestua does not fit the ozone isotopologues and is the only station that does not do it. We have clarified the section by adding the common parameters in Table 2, to highlight the common parameters (see comment Referee#3), and the differences at Harestua appear then clearly.

p.24630, lines 20-25. Is it know that the homogenization of the two records for Wollongong has been made to remove any step functions associated with the use of two different instruments that have unknown spectral characteristics?

Unfortunately, they were only 6 days of measurements with both instruments measuring simultaneously. It is too few to apply a correction based on direct comparisons. As the ILS is fitted for the Bomem spectra (so not fixed to ideal), one could expect that the ILS is correctly represented by the fitted values so that the ozone amounts are well determined. This is why we do not specify anything for the Wollongong time-series. An argument against the use of the ozone absorption line shape to retrieve simultaneously the ozone profiles and the ILS is that a change on the ozone concentration at a given altitude may be interpreted wrongly as a change in the ILS. It was found that at Jungfraujoch fitting the ILS instead of assuming that it is ideal, improved the agreement with correlative ozone profiles measurements (Barret et al., 2002). But the situation may differ at Wollongong and it would be indeed worth making careful comparisons there. Another solution to deal with periods without cell measurements, would be to retrieve independently the ILS using N₂ and CO₂ lines in the historical solar spectra, and then fix the derived ILS values during the ozone retrievals.

The control of the quality of the measurements can also be done such as in the recent paper of Barthlott (AMTD, 2014) making use of the measured XCO₂.

Discussion about the ILS has been added in the text (see also comment Referee#3).

p. 24631, line 19 – It would be good to provide additional AK from another stations for comparisons, the one that is a different in vertical distribution.

We have added a plot of the AK at Izaña.

p.24633, lines 8-9, you stated that “To reduce the auto-correlation in the residuals, we use here the monthly means time series.” The autocorrelation for monthly mean ozone time series is still significant (see estimated by Bruner et al, send of section 2) and thus affects the uncertainty of trend analysis.

Indeed, the monthly means reduces the auto-correlation, but it is still significant. That is why we also used a Cochrane-Orcutt transformation to have better estimate of the uncertainties on the trends. This

was explained at p. 24636, l. 5-8. To clarify this, we have moved this small paragraph on Cochrane-Orcutt transformation, to make it appear just after the text on monthly means.

p.24634, lines 18, 24-28, p 24635, lines . The explanation for the ELL, ELS and ELU abbreviation is not provided the first time these parameters appear in the text. Few sentences later these proxies are related to the low, middle and upper stratospheric layers. However the layers are also not clearly defined in the text. I found the description of layers in Table 3, which should be discussed a bit more in section 2.3, and the LowS, MidS and UppS should be defined there as well.

Done.

Also, please provide ftp reference for the NCEP dataset in Table 4.

We prefer not to include NCEP in Table 4, since NCEP data are not used as a proxy (except for tropopause pressure whose ftp reference is already in Table 4) and since the purpose of Table 4 is to summarize all proxies that have been tested.

p. 24635, lines 3-10 . As your trend fitting model follows the Brunner et al (2006) approach for an accumulation process over a year, please clarify if you use different tau constant for different stations (tropics vs high latitude station) and seasons.

Indeed, I also follow Brunner et al. (2006) work in using different tau constant depending on season and station. This has been clarified in the new manuscript.

p.24637, line 9-10 when describing difference in Harestua trends, add “(results are not shown)” However, it might be better to add Harestua tropospheric ozone data in Figure 5. for visual comparisons with Ny-Alesunds.

The plot for Harestua tropospheric columns has been added to Fig. 5. And we have added the text that at Thule the trend in the troposphere also occurs in the 2004-2012 period (but the plot is not shown).

p.24637 line 11-14. It is not relevant to compare ozone-sonde trends at 500 hPa level and Ny-Alesund’s integrated tropospheric column (ground to 10 km) as upper troposphere (between 500 hPa and tropopause) can have a significant contribution to tropospheric ozone column variability.

The work of Hess and Zbinden (2013) linked the ozone variability at 500 hPa (about 5-6 km) to the ozone variability observed in the lower stratosphere at 150 hPa (13-14 km), and they studied the influence of stratospheric variability on tropospheric ones. So, indeed the upper troposphere is probably linked also to ozone at 500 hPa. We believe that we can expect that the whole tropospheric column at Ny-Alesund can show similar patterns as sondes at 500 hPa since the measurements are sensitive to the ozone variability occurring in the whole column, so at 500 hPa (and up to tropopause) as well. Hess and Zbinden showed similar patterns in the 500 hPa and 150 hPa ozone at northern Europe stations, in particular in 2005. We wanted to point out that we also see the correlation between a stratospheric

influence (via VPSC proxy) and the tropospheric column at Ny-Alesund, also in 2005. To clarify that there is a connection between Trop and LowS columns at Ny-Alesund, we have added in Fig. 5 the plot for LowS, together with the associated VPSC proxy.

However, in addition to the different altitude, a difficulty of linking the work of Hess and Zbinden (2013) to ours is due to their 12-month running means which highlight the long-scale processes while we use monthly means and therefore show the month-to-month ozone variability. We have removed the comparison with this work to simplify the discussion on our own results.

p.24637, lines 18-20. I cannot see any large signal in VPSC data in 1998 and 1999. Is that what you are trying to attribute to observing larger ozone values as compared to other time periods? And it is in the contrast to 2005 and 2011 when VPSC signal is large, while tropospheric ozone is low, correct? May be this section should be re-written to make it more clear for the reader to see how VPSC might be influencing the tropospheric ozone variability at Ny-Alesund. It seems that comparison to other paper makes it difficult to understand your results.

Indeed, the larger ozone values in 1998 and 1999 were related to the VPSC, not in the sense that VPSC shows large values those years, but in the sense that it shows “non-large” values, i.e. there was less decrease of ozone those years (warm winters). So, the “regular” ozone cycle with maximum in spring (Fig. 3) is not decreased due to VPSC those years. However, in addition to the effect of “no-decrease due to VPSC” (about $+3E16$ molec.cm⁻² in Fig. 5), the QBO signal also contributes to higher values in 1998 and 1999. We will focus in the new manuscript to the 2005 and 2011 years to clarify the main message.

p.24638 line 1-3. I do not see large departure in VPSC in 2003. Moreover, the model did not capture low ozone point in 2003 (middle panels of Figure 5). May be something else can explain this variability, QBO or Equivalent latitude?

Indeed, the VPSC in 2003 is not as large as in 1996, 2000, or 2005. It is larger than 1998, 1999, or 2004, and similar to e.g. 2010. However the model gives similar ozone LowS values in 2000 and in 2003, instead of twice larger values in 2000. This is due to the TP signal (lower panel of Fig. 5) which enhances ozone values in 2000 while it decreases, in addition to VPSC, the ozone in 1996, 2005, and also in 2003, but for one single point (therefore maybe less clear in the plot). The low ozone value obtained by the model in 2003 (similar values than 2000) is due for about $1.5E17$ molec.cm⁻² to the VPSC signal and for about $4.5E17$ to the TP signal. Since the TP signal dominates the ozone decrease in 2003, we will remove from the text the reference to the 2003 year when discussing the influence of VPSC.

The measured lowest value in 2003 is indeed not captured by the model, which is only represented by VPSC and TP (Fig. 4), which means that the other proxies (including QBO and EL) were found non-significant. We have tested to run the model forcing the QBO and the EL to be included, but as might be expected (otherwise probably the proxy able to describe such a outlier event would have been significant) they do not explained the lowest value. The EL signal goes on the other direction (increases ozone at that date), while the QBO signal is too small at that date to impact significantly the ozone values. This measured low ozone value remains unexplained at present.

p.24640, lines16-17. It is hard to believe that the Lauder dataset could contain a significant contribution from Solar cycle, especially in the troposphere. As authors point out – the record is too short to be analyzed for a Solar cycle signal. I would not use the Solar cycle in analysis, or would adapt

the fit from another middle latitude station (i.e. Wollongong?). You can try to analyze a shortened 2001-2012 record from Wollongong to check if you get similar artifact from fitting data with the Solar cycle proxy .

We have made the analysis at Wollongong for the 2001-2012 period, and the time-series (therefore the solar cycle signal) do not show the same behavior as in Lauder. To stay coherent for all stations, we prefer to keep the model the same for all stations, but we have highlighted even more than in the previous manuscript that the solar signal should be taken with care at Lauder: we give the trends without the solar cycle in Table 6. The impact is not large in MidS and Total columns, but the 1.1 %/decade decrease on UppS trend is sufficient to make the trend non-significant (+1.7+/-2.4 compared to +2.8 +/-2.4).

p.24641, line20-24. Can the choice of 470 K reanalysis for calculation of the ELL for Wollongong be a problem or is it a sequential model fit that determines which proxy to keep? Why was 470K chosen to represent the low stratospheric layer at Wollongong?

For each layer, the initial model starts with only the seasonal cycle and the trend parameters. Then the choice of the proxies to be added in the model is made by a stepwise regression procedure as described in Sect. 3. The model tests all given proxies (solar, QBO, TP,...). For the EL proxy we test in the model only the EL proxy that corresponds to the altitude of the approximate middle of the layer. Therefore, it is not possible to include the ELM or ELU proxies in the model for the LowS columns. For the total columns, the three ELL, ELU and ELM proxies are tested.

Concerning the choice of 460 K for ELL at Wollongong and Izana: we make an approximation with the Equivalent Latitude used for the different layers. We are dealing with thick partial columns: 12-20 km for high and mid latitude stations; 15-23 km for subtropical stations, to avoid to be too close to the tropopause region which could include tropospheric signal in the lower stratospheric layer. So, we have chosen to use the Equivalent Latitude which would correspond to approximately the altitude of the middle of the layer (about 16 km and 19 km, for mid/high and subtropical latitudes, respectively). Indeed, for Wollongong the choice of 460 K has an impact on the trend of LowS: if we use the 370 K proxy, there is no trend anymore in the proxy itself and the Wollongong LowS trend becomes +2.5+/-2.8 %/decade. The impact of using the 370/550/950 K series instead of the 460/700/1040 K is negligible at Izana and at Wollongong for the other layers. We prefer therefore to stay coherent with the way we have chosen the EL proxy, and provide to the reader the information about the trend in the EL proxy at 460 K, and the obtained trend at Wollongong without this proxy (+2.4+/-2.8 %/decade), in case one would like to remove this impact for comparisons. Probably, the way of dealing with the EL proxies could be improved in the future.

Answers to Referee#3

We thank the referee for his/her constructive remarks and suggestions. We answer below to the specific comments.

The phrase ‘self-calibrated’ is used in both the introduction and conclusions. Although the optical absorption due to ozone is measured with reference to the surrounding continuum there are a number of steps from this to derive a vertical profile of ozone, many of which are not ‘self-calibrating’. The measurements made by the different sites are linked to a common spectroscopic database, but since different absorption lines are used, the absolute accuracy of the actual spectral parameters used could be different; the analysis requires P&T profiles and any errors on these will affect the results; and changes/differences in instrumental performance (e.g. effective resolution, phase, etc.) could affect profile results. Significantly more justification is therefore needed before the data can be said to be ‘self-calibrated’.

The referee is right. We used the term “self-calibrated” because the ozone columns measurements are repeatable and stable over time (if the same spectroscopic parameters is used, or model parameters in general), i.e., the technique of measurement itself would not change the ozone column that would be derived from two measurements with the same ozone amount in the atmosphere. However, for long-term series when the ILS can possibly change between the measurements, this indeed would not be true. Therefore, we have added in the Introduction and Conclusion Sections that a careful treatment of the ILS is required to obtain reliable ozone values and trends. This is especially true for the partial columns, the impact of the ILS being smaller on total columns.

Concerning the common spectroscopic database, but different absorption lines: the spectroscopic parameters have an impact on the systematic uncertainty of individual measurements. Therefore, if a bias can be obtained in the ozone amounts at one station by using slightly different or additional micro-windows, it would be systematic for the long-term series and therefore it would not imply different trend results. But, indeed, if there is a drift in the p&T profiles, this could influence the trends differently in case of different micro-windows used. We have made the test of using at Kiruna the same 1000-1005 cm^{-1} as at other stations. The trends are very similar than with the settings used in the paper (Trop: -1.1 ± 2.5 %/dec. (instead of: -0.9 ± 2.5); LowS: -3.4 ± 2.5 (-3.9 ± 2.6); MidS: -0.0 ± 2.4 ($+0.4 \pm 2.6$); UppS: $+6.6 \pm 3.1$ ($+7.4 \pm 3.4$); TotCol: -0.3 ± 1.5 (-0.3 ± 1.6). At Ny-Alesund, the approach of using only the 1000-1005 cm^{-1} window has also been tested, with again a little change on the trends well below the uncertainty on the trends (1.4%/dec. impact on Trop trend, and less than 0.7 %/dec. for the other partial/total columns). The conclusions on these tests have been added in the new manuscript in the Sect.2.2 where the impact on the different parameters on trends are more discussed (according to the Referee’s next comment).

Concerning the possible errors on the p&T profiles: the random uncertainties due to the temperature are taken into account in the uncertainty budget. If the NCEP temperature data contain a drift of 1%/decade, which seems not excluded from e.g. the analysis of D. Hubert on the impact of NCEP p&T on SAGE-II v6.2 ozone drift (Hubert et al., in preparation for AMT), our uncertainties on single station trends of about 2%/decade would increase up to only 2.2%/decade if this systematic temperature component would be included (Daan Hubert, personal communication).

Section 2.2 describes the FTIR retrieval strategy, and one common theme is that there are very few aspect of the retrieval that are common to all groups. While the differences are acknowledged there is very little discussion of the reason for the differences or the potential influence these differences

could have (either on the absolute values of the ozone data or on the trends derived). Without further discussion on this point it is difficult to know how much reliance can be placed on the differences in the results from difference sites being due to the atmosphere and how much to the differences in the analysis strategies. Some further analysis that actually assessed some of the implications of the different strategies would significantly enhance the robustness of the results and conclusions.

We have added more discussion in Sect.2.2 on the reason for the differences and on the influence of the differences on the trends.

The two parameters that could have a significant impact on the trends is the micro-windows, if the p&T NCEP profiles contain long-term drift; and the treatment of ILS. For the former, the test has been made at Kiruna and Ny-Alesund to use the 1000-1005 cm^{-1} window, and it has been found that this does not impact the trends significantly (see previous comment). Due to the small impact of this parameter, the time-series analyses have not been updated with a unique choice of micro-window for the present paper, but this is a parameter which will be easily homogenized in future work.

For the ILS treatment, the individual choices were led by the type of spectrometer and the availability of cell measurements: Bruker 120M and Bomem are not stable enough to allow to use a fixed ideal ILS. Therefore, the LINEFIT results were used at stations where the HBr cell measurements were made (so not possible for the old Bomem spectra). At Jungfraujoch, the cell measurements started only in the early 2000's, so to stay homogeneous they used a fitted eap parameter for the whole time-series. We have tested the impact of fitting the eap instead of using an fixed ideal ILS at Ny-Alesund, and again little impact have been found on the trends (less than 0.6%/decade for all layers).

The determination of the ILS (pg 24630) is obviously important, particularly in the profile retrieval and long-term changes/drifts in the ILS could presumably map onto the trend results. There is a description of the ILS procedures followed but several times results are referred to as being 'close to' the ideal and therefore assumed to be ideal. It is important to know what is the definition of 'close to' is in each of these cases and how this criteria was selected. It would also be useful to know how often the ILS checks are done as this would cover the issue of potential long-term alignment drift.

We have highlighted more the importance of ILS in the new manuscript (Introduction, Sec. 2.2 and Conclusion). The discussion about the ILS treatment in Sect 2.2. has been updated to provide more information (also see the response to the Referee#1 comment on Wollongong time-series). The ILS was assumed to be ideal if the loss of modulation efficiency at maximum OPD is below 2%. The frequency of the ILS checks is at least every 6 months for the Bruker 120/125 HR instruments used in the present study. But it can be more often for other stations (e.g. at Izaña, see García et al., 2012).

We have clarified the reason for the different choices of ILS and we have made the test at Ny-Alesund to change the treatment of ILS (see previous comment).

It would be useful to have further details on the sensitivity in Section 2.3. Although fig 1 shows the sensitivity profile for the Jungfraujoch station, it would be interesting to know something about the overall sensitivity for each of the four altitude layers for each station being analysed as this would indicate the potential influence of trends in the a priori data on the analysis.

We have added a plot for the Izaña station, since the layer limits are slightly different for this station, and since the calculated sensitivity is different because of the use of Tikhonov regularization instead of optimal estimation. We do not want to add plots for all stations to minimize number of pages / plots. But

we have added a sentence in the manuscript: “Similar averaging kernels are obtained at each station (not shown).” For all stations (so even for Izaña and Kiruna that are using Tikhonov regularization), the DOFS above 49 km is small (from 0.006 for Jungfrauoch to 0.04 for Izaña).

Specific comments :

Page 24626 Line 14 : ‘stable data are needed’ – it is not the data that needs to be stable. Suggest replace with ‘reliable data from stable instruments are needed’.

Done.

Page 24626 Line 16. Do ozonesondes count as ‘ground-based’ or are they ‘in-situ’ measurements ?

The idea was to oppose “ground-based” to satellite, but it is of course “technically” not correct. So we changed the text. “Ground-based (Dobson, Umkehr) and ozonesondes data are traditionally used for these studies...”

Page 24628 Line 19. Should it be ‘single scaling’ or ‘simple scaling’ ? ‘apriori’ is missing a space and should it be in italics (throughout document) ?

Indeed, we meant “simple”: changed.

We prefer to let “a priori” in normal text, it is commonly used now.

Page 24629 Line 17. This assumption implies there is no correlation from the measurement noise in the vertical information. This seems a large assumption to make without any further justification. Some more discussion on this point would be useful.

The measurement noise matrix S_g (dimension: $m \times m$, m being the number of points in the discretized measured spectrum y) is assumed diagonal meaning that we expect no correlation between the noise at different wavelengths (which is indeed an approximation but it is quite common, Rodgers 2000). Then, the measurement noise error matrix S_n is calculated with $S_n = G S_g G^t$, with G the gain matrix= $\delta x / \delta y$, x the retrieved state, y the measurement. So the measurement noise error S_n is not diagonal, meaning that there is indeed some correlation in the measurement noise error between altitude layers.

Page 24631 Line 12. If the sensitivity is the fraction from the measurement rather than the a priori, how can it be greater than 1 (see Fig 1) ?

The sensitivity is not “mathematically” the fraction between measurement and a priori. We have change the sentence to “the sensitivity ... represents **roughly** the fraction of the retrieval that comes from the measurement rather than from the a priori information”. The sensitivity is good (information is coming from the measurement) when it is close to 1 (Rodgers, 2000). It can happen (Rodgers, 2000) that it is greater than 1 (area of the averaging kernel at this altitude is greater than 1), showing that at this altitude the retrieved profile might be too sensitive to a change on the true state.

Page 24631 Line 21. The sensitivity shown in Fig 1 is >0 at 49 km, so what was the actual cut-off criteria ?

Again “goes to zero” was a language approximation, we meant “becomes negligible”, not strictly zero. For the upper layer, we could use, as an upper limit, the last layer of the retrieval grid, which is 100 or

120 km, depending on the station. Having a layer 29-100 km, may be misleading: one could think that FTIR measurements are sensitive to ozone changes up to 100 km. We have decided to take a cut-off criteria above which the DOFS are very small. In the optimal estimation method of regularization, this coincide with a sensitivity close to zero. However, as shown in the new plot of the Izaña averaging kernels, the sensitivity when Tikhonov regularization is used does not decrease to zero with height, as the DOFS does. So in our case, the 49 km cut-off, coincide with a DOFS above this altitude that are between 0.006 (for Jungfraujoch) to 0.04 (for Izaña).

The precise values (49 instead of 50 km; 29 instead of 30 km), are due to the retrieval grids of the stations. Each station has between 44 and 47 layers of varying widths (more layers in the troposphere than in the upper stratosphere), and we have chosen the limits of the 4 partial columns to coincide with some selected limits (based in DOFS) of the stations grids, to avoid interpolations.

Page 24632 Line 7. 'UV-VIS' rather than 'UV-VIS'.

Done.

Page 24632 Line 22. Suggest 'variable' rather than 'contrasted'.

Done.

Page 24633 Line 16. Parameter A0 is not defined.

Done.

Page 24633 Line 18 (and eq 2) should it be "(t) rather than just " ?

Done.

Page 24634 Line 22 Clarify which ones 'those proxies' refers to.

Done.

Page 24639 Line 17. As the total column results as also given in DU in section 4.2.5 it would be good to also do so here.

Done.

Page 24645 Line 28. Does 8 sites constitute 'many' for a global network ? Suggest replace with the actual number.

Only 8 stations have contributed to the present paper. However, more stations could contribute after re-analysis of their time-series, using the described retrieval strategies (Arrival Heights, Rikubetsu, Eureka, Bremen). Some were suffering from gaps in the measurements but could be used in the future when/if more years of data will become available (Mauna Loa, Rikubetsu). We have added this information in the manuscript.

Page 24646 Line 4. Suggest replace 'proposed' with 'demonstrated'.

Done.

Trends of ozone total columns and vertical distribution from FTIR observations at 8 NDACC stations around the globe

C. Vigouroux¹, T. Blumenstock², M. Coffey³, Q. Errera¹, O. García⁴, N. B. Jones⁵, J. W. Hannigan³, F. Hase², B. Liley⁶, E. Mahieu⁷, J. Mellqvist⁸, J. Notholt⁹, M. Palm⁹, G. Persson⁸, M. Schneider⁴, C. Servais⁷, D. Smale⁶, L. Thölix¹⁰, and M. De Mazière¹

¹Department of Atmospheric Composition, Belgian Institute for Space Aeronomy (BIRA-IASB), Brussels, Belgium

²Karlsruhe Institute of Technology (KIT), Institute for Meteorology and Climate Research (IMK-ASF), Karlsruhe, Germany

³Atmospheric Chemistry Division, National Center for Atmospheric Research (NCAR), Boulder, Colorado, USA

⁴Izaña Atmospheric Research Centre (IARC), Agencia Estatal de Meteorología (AEMET), Santa Cruz de Tenerife, Spain

⁵Centre for Atmospheric Chemistry, University of Wollongong, Wollongong, Australia

⁶Department of Atmosphere, National Institute of Water and Atmospheric Research Ltd (NIWA), Lauder, New Zealand

⁷Institute of Astrophysics and Geophysics, University of Liège (ULg), Liège, Belgium

⁸Department of Earth and Space Science, Chalmers University of Technology, Göteborg, Sweden

⁹Institute of Environmental Physics, University of Bremen, Bremen, Germany

¹⁰Climate Research, Finnish Meteorological Institute (FMI), Helsinki, Finland

Abstract. Ground-based Fourier transform infrared (FTIR) measurements of solar absorption spectra can provide ozone total columns with a precision of 2 %, but also independent partial column amounts in about four vertical layers, one in the troposphere and three in the stratosphere up to about 45 km, with a precision of 5–6 %. We use eight of the Network for the Detection of Atmospheric Composition Change (NDACC) stations having a long-term time series of FTIR ozone measurements to study the total and vertical ozone trends and variability, namely: Ny-Alesund (79° N), Thule (77° N), Kiruna (68° N), Harestua (60° N), Jungfraujoch (47° N), Izaña (28° N), Wollongong (34° S) and Lauder (45° S). The length of the FTIR time-series varies by station, but is typically from about 1995 to present. We applied to the monthly means of the ozone total and four partial columns a stepwise multiple regression model including the following proxies: solar cycle, Quasi-Biennial Oscillation (QBO), El Niño-Southern Oscillation (ENSO), Arctic and Antarctic Oscillation (AO/AAO), tropopause pressure (TP), equivalent latitude (EL), Eliassen-Palm flux (EPF), and volume of polar stratospheric clouds (VPSC).

At the Arctic stations, the trends are found mostly negative in the troposphere and lower stratosphere, very mixed in the middle stratosphere, positive in the upper stratosphere due to a large increase in the 1995–2003 period, and non-significant when considering the total columns. The trends for mid-latitude and subtropical stations are all non-significant, except at Lauder in the troposphere and upper stratosphere, and at Wollongong for the total columns and the lower and middle stratospheric columns, where they are found positive. At Jungfraujoch, the upper stratospheric trend is close to significance ($+0.9 \pm 1.0$ % decade⁻¹). Therefore, some signs of the onset of ozone mid-latitude recovery are observed only in the Southern Hemisphere, while a few more years seems to

be needed to observe it at the northern mid-latitude station.

1 Introduction

While the past negative trend in the ozone layer has been successfully attributed to the increase of ozone depleting substances, and reproduced by chemistry-climate models, understanding and predicting the current and future ozone layer, and especially attributing an ozone recovery to the positive effect of the Montreal Protocol and its Amendments and Adjustments, is still a challenge. This results from natural variability, observation uncertainties, and changes in dynamics and temperature induced by the increase of greenhouse gases (WMO, 2010). Long-term measurements of total and vertical ozone are required to understand the ozone response to different natural and anthropogenic forcings. Since the long-term satellite experiments ceased to operate (i.e. SAGE, HALOE), the satellite community is working on merging the past records to the new measurements performed by a number of satellite instruments launched since 2000 (e.g. Bodeker et al., 2013; Kyrölä et al., 2013; Sioris et al., 2014; Chehade et al., 2014). Reliable data from stable instruments are needed to validate these satellite extended datasets, and to offer an alternative determination of ozone total and vertical changes. Ground-based (Dobson, Umkehr) and ozonesondes data are traditionally used for these studies, already reporting trends in the 1985 ozone report (WMO, 1985), followed in 1998 by Lidar and microwave measurements (WMO, 1998). Ground-based FTIR (Fourier Transform Infra-Red) measurements derived from high-resolution solar absorption spectra provide an additional ozone data set, and they have been used for trend studies for the first time in Vigouroux et al. (2008) with 10 years of data (1995–2004) at several European stations, then updated in the WMO (2010) report. Additional similar studies have been performed at individual stations (Mikuteit, 2008; García et al., 2012). These measurements

have their own advantages. First, for atmospheric gases such as ozone which have very narrow absorption lines, the ozone absorption signatures are self-calibrated with the reference being the surrounding continuum. Therefore, the derived absolute ozone columns depend mainly on the employed spectroscopic parameters which dominate the systematic uncertainty budget. Second, they can provide not only ozone total columns with a precision of 2%, but also low vertical resolution profiles, obtained from the temperature and pressure dependence of the absorption line shapes. This leads to about four independent partial columns, one in the troposphere and three in the stratosphere up to about 45 km, with a precision of about 5–6%. The instrumental line shape (ILS), which depends on the alignment of the spectrometer, impacts the absorption line shape on which is based the ozone profile retrievals. Hence, it is important to have an accurate knowledge of the ILS in order to derive correct ozone profiles and trends.

The work discussed in this paper expands the previous study of Vigouroux et al. (2008): it is based on longer time series, it includes FTIR data from stations outside Europe, and it uses a stepwise multiple linear regression model including several explanatory variables for the trend evaluation. It is presented as follows: Sect. 2 provides information about the FTIR ozone observations (retrieval strategies, characterization of the vertical information, time series and seasonality). Section 3 describes the stepwise multiple linear regression model applied to the ozone time series. Section 4 presents and discusses the trend results, as well as the explained part of ozone variability. Section 5 summarizes the conclusions.

2 Ground-based FTIR ozone observations

2.1 FTIR monitoring

Table 1 identifies the ground-based FTIR stations, all part of NDACC (Network for the Detection of Atmospheric Composition Change), that are contributing to the present work. The latitudinal coverage is good: from 79° N to 45° S. These stations perform regular solar absorption measurements, under clear-sky conditions, over a wide spectral range (around 600–4500 cm⁻¹) and the derived time series of total column abundances of many atmospheric species are available in the NDACC database (<http://www.ndacc.org>). While the stations are all currently active, they started their regular monitoring activities at different times. The period of measurement used for ozone trend analysis at each station is summarized in Table 1, together with the instrument manufacturer and type. Some of the stations performed measurements even earlier but these older spectra, taken with different spectrometers have to be carefully re-analysed first before being included in a trend study. The instruments currently used are the high-resolution spectrometers Bruker 120 M, 125 M,

120 HR, and 125 HR which can achieve a spectral resolution of 0.0035 cm⁻¹ or better. The Bomem DA8 used in the first years of Wollongong measurements has a spectral resolution of 0.004 cm⁻¹.

2.2 FTIR retrieval strategy

We refer to Vigouroux et al. (2008) for more details on the ozone FTIR inversion principles, which are based on the optimal estimation method (Rodgers, 2000). The effort of retrieval homogenization initiated in Vigouroux et al. (2008) has been pursued and we report in Table 2 the common retrieval parameters. The spectroscopic database has been updated to HITRAN 2008 (Rothman et al., 2009). All stations are employing the daily pressure and temperature profiles from NCEP (National Centers for Environmental Prediction). A common source for the ozone a priori profiles is used: the model WACCM4 (Garcia et al., 2007) calculated at each FTIR station, except at Harestua where a climatology based on ozonesondes and HALOE measurements is used. Finally, the interfering species fitted in the ozone retrievals, usually with a simple scaling of their a priori profile, are the same for all stations, namely, H₂O, CO₂, C₂H₄, and the ozone isotopologues ⁶⁶8O₃ and ⁶⁸6O₃. Only Harestua do not fit C₂H₄ and the ozone isotopologues.

Some retrieval parameters still differ from station to station, either for historical reason or for the inherent specificities of the different locations. They are also summarized in Table 2.

First, two different profile retrieval algorithms are widely used depending on each team expertise, PROFITT9 (Hase, 2000) at Kiruna and Izaña, and SFIT2 (Pougatchev et al., 1995) at the six other stations. It has been demonstrated in Hase et al. (2004) that the profiles and total column amounts retrieved from these two different algorithms under identical conditions are in excellent agreement.

Second, the micro-windows sets involve some common lines at all stations, which ensures that only small bias is expected due to the different micro-windows choices. Either some additional thin micro-windows are used together with the 1000–1005 cm⁻¹ or, at Kiruna and Izaña, a different choice was led by the priority given to avoid the more intense H₂O lines while having still a high DOFS. All choices of micro-windows lead to the required 4 to 5 Degrees of Freedom for Signal (DOFS), thanks to the numerous ozone lines with different intensities which give information both in the stratosphere and the troposphere. The test has been made at Kiruna and Ny-Alesund to use the 1000–1005 cm⁻¹ window only and, as expected, only little impact has been observed: except for Ny-Alesund tropospheric trends (1.4%/decade), we obtained small trend differences between 0.0 and 0.8%/decade, which is in all cases well below the uncertainty on the trends (see Section 4). However, it is planned, within the InfraRed Working Group of NDACC, to fix a common choice of micro-windows for future improved homogenization.

Table 1. Characteristics of the FTIR stations that are contributing to the present work: location and altitude (in km a.s.l.), time-period covered by the ozone measurements used in the present trend analysis, and instrument type.

Station	Latitude	Longitude	Altitude (km)	Time-period	Instrument
Ny-Alesund	79° N	12° E	0.02	1995–2012	Bruker 120 HR
Thule	77° N	69° W	0.22	1999–2012	Bruker 120 M
Kiruna	68° N	20° E	0.42	1996–2007	Bruker 120 HR
				2007–2012	Bruker 125 HR
Harestua	60° N	11° E	0.60	1995–2009	Bruker 120 M
				2009–2012	Bruker 125 M
Jungfraujoch	47° N	8° E	3.58	1995–2012	Bruker 120 HR
Izaña	28° N	16° W	2.37	1999–2005	Bruker 120 M
				2005–2012	Bruker 125 HR
Wollongong	34° S	151° E	0.03	1996–2007	Bomem DA8
				2007–2012	Bruker 125 HR
Lauder	45° S	170° E	0.37	2001–2012	Bruker 120 HR

Third, the main interfering species in this spectral region is water vapor, and it has been dealt with differently depending on the station: at Wollongong and Lauder station, the H₂O profile is retrieved simultaneously with the ozone profile, adding the micro-window 896.4–896.6 cm⁻¹ for a better H₂O determination. At Kiruna, Izaña and Jungfraujoch, the H₂O a priori profiles are only scaled in the ozone retrieval, but these a priori profiles have been preliminarily retrieved in dedicated H₂O micro-windows for each spectrum (Schneider et al. (2006) for Kiruna and Izaña; Sussmann et al. (2009) for Jungfraujoch). For the very dry Jungfraujoch site, it has been found that preliminary H₂O retrievals do not improve the quality of the ozone retrievals. At Ny-Alesund and Thule, water vapor is treated as the other interfering species: only a scaling of a single a priori profile from WACCM4 is made. **Therefore, except at the two latter stations, the H₂O profile variability has been well taken into account. This may be a future improvement to be done in Ny-Alesund and Thule strategies. However, the random uncertainties due to the water vapor interference are not dominating the ozone error budget (see Sect. 2.3), and we expect a negligible impact on the ozone trends due to the H₂O treatment.**

Fourth, the choice of the regularization (a priori covariance matrix, \mathbf{S}_a , and Signal to Noise Ratio, SNR) cannot be easily homogenized because it depends on the real variability of ozone which is different at each station location and on the real SNR achieved by each spectrometer. In optimal estimation, the choice of the a priori covariance matrix \mathbf{S}_a is an important parameter of the inversion process, and together with the measurement noise error covariance matrix \mathbf{S}_ϵ , it will lead to the following averaging kernel matrix \mathbf{A} (Rodgers, 2000):

$$\mathbf{A} = (\mathbf{K}^T \mathbf{S}_\epsilon^{-1} \mathbf{K} + \mathbf{S}_a^{-1})^{-1} \mathbf{K}^T \mathbf{S}_\epsilon^{-1} \mathbf{K}, \quad (1)$$

where \mathbf{K} is the weighting function matrix that links the measurement vector \mathbf{y} to the state vector \mathbf{x} : $\mathbf{y} = \mathbf{K}\mathbf{x} + \epsilon$, with ϵ representing the measurement error. In our retrievals, we

assume \mathbf{S}_ϵ to be diagonal, in which case the diagonal elements are the inverse square of the SNR. The diagonal elements of \mathbf{S}_a represent the assumed variability of the target gas volume mixing ratio (VMR) at a given altitude, and the non-diagonal elements represent the correlation between the VMR at different altitudes. We can see in Table 2 that, except at Harestua, Kiruna and Izaña, the stations are using an a priori covariance matrix with diagonal elements constant with altitude corresponding to 10, 20 or 30 % variability, the largest variability taking place at the high latitude stations Ny-Alesund and Thule. At Harestua, the diagonal elements of \mathbf{S}_a correspond to 11 % in the stratosphere, decreasing down to 6 % in the troposphere and to 5 % above 35 km. Except at Ny-Alesund, the SNR value is not the real one coming from each individual spectrum, but an effective SNR, that is used as a regularization parameter. This effective SNR is smaller than the value derived from the inherent noise in the spectra, since the residuals in a spectral fit are not only coming from pure measurement noise but also from uncertainties in the model parameters. At Kiruna and Izaña, the regularization is made using the Tikhonov L1 constraint (Tikhonov, 1963). **The regularization choice (\mathbf{S}_a and SNR) is made at each station in order to obtain stable retrievals with reasonable DOFS. The regularization, via the \mathbf{A} matrix, will impact, together with the real natural variability of ozone, the smoothing uncertainty which is the dominant source for the tropospheric and lower stratospheric columns. However, this is mainly a random uncertainty source and it as been shown at Izaña that using Tikhonov regularization or a \mathbf{S}_a matrix obtained from ozone climatological measurements do not impact the ozone trends significantly (García et al., 2012).**

The last important parameter is the instrumental line shape (ILS). As already mentioned, the ILS impacts the absorption line shape on which is based the ozone profile retrievals. Hence, if it is not properly included in the forward model or in the retrieval process, and if the alignment of the in-

Table 2. Summary of the ozone retrieval parameters. All micro-window (mw) limits are given in cm^{-1} . Ny: Ny-Alesund; Th: Thule; Ha: Harestua; Ju: Jungfraujoch.

Parameters	Ny-Alesund/Thule	Harestua/Jungfraujoch	Kiruna/Izaña	Wollongong/Lauder
Spectroscopic database	HITRAN 2008	HITRAN 2008	HITRAN 2008	HITRAN 2008
Pressure and temperature	NCEP	NCEP	NCEP	NCEP
Ozone a priori profiles	WACCM4	WACCM4 (Ju) climatology based on sondes and HALOE (Ha)	WACCM4	WACCM4
Retrieval code	SFIT2 ^a v3.94	SFIT2 ^a v3.94	PROFFIT9 ^b	SFIT2 ^a v3.94
Micro-windows	1000–1005 782.56–782.86 (Ny) 788.85–789.37 (Ny) 993.3–993.8 (Ny)	1000–1005	991.25–993.80 1001.47–1003.04 1005.0–1006.9 1007.347–1009.003 1011.147–1013.553	1000–1005 782.56–782.86 788.85–789.37 993.3–993.8 896.4–896.6 (H ₂ O)
Interfering species	H ₂ O, CO ₂ , C ₂ H ₄ , ⁶⁶⁸ O ₃ , ⁶⁸⁶ O ₃	H ₂ O, CO ₂ , C ₂ H ₄ , ⁶⁶⁸ O ₃ , ⁶⁸⁶ O ₃ (Ju) H ₂ O, CO ₂ (Ha)	H ₂ O, CO ₂ , C ₂ H ₄ , ⁶⁶⁸ O ₃ , ⁶⁸⁶ O ₃	H ₂ O, CO ₂ , C ₂ H ₄ , ⁶⁶⁸ O ₃ , ⁶⁸⁶ O ₃
H ₂ O treatment – a priori profile	One single profile (Ny) Preliminary retrievals in dedicated H ₂ O mws (Th)	One single profile (Ha) Preliminary retrievals in dedicated H ₂ O mws (Ju)	Preliminary retrievals in dedicated H ₂ O mws	One single profile
– fit in ozone mw	Scaling retrieval only	Scaling retrieval only	Scaling retrieval only	Profile retrieval
Regularization: – S _a	Diagonal: 20 % (Ny) Diagonal: 30 % (Th) No inter-layer correlation	Diagonal: 5 to 11 % (Ha) Diagonal: 10 % (Ju) No inter-layer correlation (Ha) Inter-layer correlation: gaussian decay 4 km (Ju)	Tikhonov regularization L1	Diagonal: 10 % Inter-layer correlation: exponential decay 4 km
– SNR	Real SNR (depending on each spectrum), except ^c regions at: 1000.85–1001.45 1003.16–1004.5 set to SNR = 1 (Ny) Constant = 50 (Th)	Constant = 100 (Ju) Constant = 200 (Ha)	Depending on each spectrum	Constant = 150
Instrumental Line Shape	Fixed ideal (Ny) Fixed from LINEFIT (Th)	Fixed from LINEFIT (Ha) 2nd order polynomial fit of (Ju)	Fixed ideal (Kiruna) Fixed from LINEFIT (Izaña)	Fixed ideal except Bomem spectra: 4th order polynomial fit of EAP

^a Pougatchev et al. (1995);^b Hase (2000);^c in order to mask strong H₂O absorptions.

strument is changing over time, this could impact the derived ozone trends (García et al., 2012). There are three options for considering the ILS and the choice is led by the type of spectrometer and the availability of cell measurements. A perfect alignment of the instrument would provide an "ideal" ILS: the modulation efficiency and the phase error remain equal to 1 and 0, respectively, along the optical path differences (OPDs). This perfect alignment can usually be achieved and maintained over time by the stable Bruker 120 or 125 HR. Even when those spectrometers are used, the alignment must be controlled by HBr or N₂O absorption measurements in a low-pressure gas cell and the use of the LINEFIT code, as described in Hase et al. (1999). In this approach, the loss of modulation efficiency and the phase error can be described (1) by 40 parameters (20 for each) at equidistant OPDs; (2) or simply by two parameters assuming a linear decline of the modulation efficiency with OPD, and a constant phase error. At all stations using the 120 or 125 HR spectrometers, and where the cell measurements were available for the whole period and taken at least twice a year (Ny-Alesund, Kiruna, Lauder, Wollongong from 2007), the ILS retrieved from LINEFIT was found good and stable: less than 2% of loss in modulation efficiency at the maximum OPD. It has been therefore considered and fixed as ideal in the forward model. For the stations where the cell measurements were available and where the ILS could not be considered ideal, which was the case for the stations running a Bruker 120 M instrument, the ILS was fixed in the forward model to the parameters obtained by LINEFIT using either option (1) at Thule and Izaña or option (2) at Harestua. At Jungfraujoch up to the early 2000's, and at Wollongong when the Bomem instrument was used, no cell measurements were performed, hence it is not possible to use the LINEFIT results in the forward model. To take into account that the ILS may not be ideal, the modulation efficiency is retrieved simultaneously with the ozone profiles, by using a polynomial fit of order 2 (Jungfraujoch) or 4 (Wollongong). The phase error has been neglected, i.e. it is treated as ideal. An argument against the use of the ozone absorption line shape to retrieve simultaneously the ozone profiles and the ILS is that a change on the ozone concentration at a given altitude may be interpreted wrongly as a change in the ILS. But it was found that at Jungfraujoch the fitting of the ILS instead of assuming that it is ideal, improved the agreement with correlative ozone profiles measurements (Barret et al., 2002), leading to the conclusions that there was enough information in the absorption line shapes to isolate correctly the ILS effect. We have made the test at Ny-Alesund to use a polynomial fit (order 2) of the modulation efficiency instead of a fixed ideal ILS. We found very small impact on the trends (less than 0.6%/decade for all layers). Of course the situation may differ for stations with worse alignment if this one cannot be reproduced by a polynomial fit of the modulation efficiency. Another solution to deal with periods without cell measurements would be to retrieve independently the ILS using N₂ and CO₂ lines

in the historical solar spectra, since these gases have very well-known vertical profiles, and then fix the ILS to these preliminary derived values in the ozone retrievals.

2.3 Vertical information in FTIR retrievals

The vertical information contained in the FTIR retrievals can be characterized by the averaging kernel matrix \mathbf{A} (Eq. 1), as described in detail in Vigouroux et al. (2008). It has been shown in this previous paper that the ozone retrievals provide 4–5 DOFS, depending on the station. Therefore, in addition to total column trends, we provide ozone trends in four independent partial column layers, corresponding to the vertical information. The layer limits have been chosen such that the DOFS is at least 1.0 in each associated partial column. The adopted layers are independent according to the resolution of the averaging kernels, as can be seen in Fig. 1, where the partial column averaging kernels of the four layers in the case of Jungfraujoch and Izaña are shown. Similar averaging kernels are obtained at each station (not shown). Also shown is the sensitivity which is, at each altitude k , the sum of the elements of the corresponding averaging kernel $\sum_i A_{ki}$, and represents roughly the fraction of the retrieval that comes from the measurement rather than from the a priori information. At Izaña, the sensitivity does not decrease towards zero at about 50 km (Fig. 1), because of the use of Tikhonov regularization instead of optimal estimation (García et al., 2012). In the present work, small changes have been made in the partial column limits in comparison to Vigouroux et al. (2008): we avoid the tropopause region at each station, in order to have a better separation between the layer that we call the "tropospheric" layer, and the lower stratospheric layer. Due to the high tropopause heights at Izaña (14.9 km) and Wollongong (13.8 km), compared to mid- and high-latitude stations (from 10.1 km at Ny-Alesund to 11.8 km at Jungfraujoch), we use different partial column limits for these two stations. The upper limit of the upper layer is here 49 km, the altitude above which the DOFS is small (from about 0.01 to 0.04 depending on station), instead of 42 km in Vigouroux et al. (2008), chosen as the altitude above which the sensitivity was below 0.5. We still gain from 0.06 (Jungfraujoch) up to 0.23 (Lauder) DOFS in this 7 km wide range with poorer sensitivity. For Harestua, the chosen layer limits give a DOFS of only 0.9 and 0.75, in the ground 10 km and in the 29–49 km layers, respectively.

We provide in Table 3, for each station, the partial column limits of the four defined layers (Trop: Troposphere; LowS: Lower Stratosphere; MidS: Middle Stratosphere; UppS: Upper Stratosphere). The detailed error budget for ozone FTIR retrievals has been described in Vigouroux et al. (2008) and more recently in García et al. (2012) for Izaña, and we just summarize in Table 3 the total random uncertainties obtained for the present choice of layers, and for the total columns (TotC). As obtained in the two previous papers, and not shown here, the smoothing error is the dominant random er-

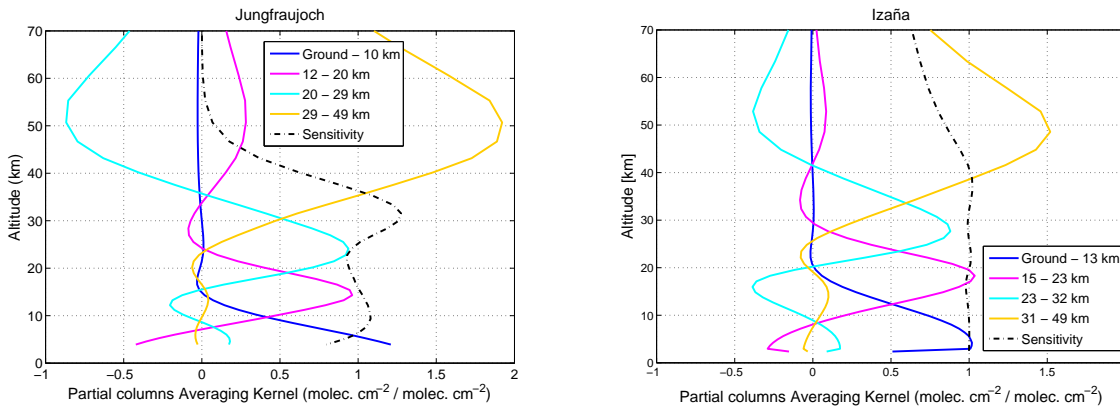


Fig. 1. Partial column averaging kernels ($\text{molec. cm}^{-2} (\text{molec. cm}^{-2})^{-1}$) for ozone retrievals at Jungfraujoch (left) and Izaña (right) stations.

Table 3. Partial column (PC) limits for the 4 altitude layers containing at least one DOFS. The random uncertainties are given for each partial column. Trop: Troposphere; LowS: Lower Stratosphere; MidS: Middle Stratosphere; UppS: Upper Stratosphere; TotC: Total Columns; Gd: Ground; Err.: Total Random Uncertainties.

Layers	Stations	PC limits	Err.
Trop	Izaña/Wollongong	Gd-13/12 km	6%
	Other stations	Gd-9/10 km	5%
LowS	Izaña/Wollongong	15–23 km	5%
	Other stations	12–20 km	4%
MidS	Izaña/Wollongong	23–32 km	5%
	Other stations	20–29 km	5%
UppS	Izaña/Wollongong	31–49 km	5%
	Other stations	29–49 km	5%
TotC	Izaña/Wollongong	–	2%
	Other stations	–	2%

ror source for the tropospheric and lower stratospheric layer, while the temperature dominates the random error budget for the middle and upper stratospheric layers, and for total columns. Also found in these two papers, and not repeated here, is the validation of the FTIR total and partial columns with correlative data (Dobson, Brewer, UV-Vis, ozonesondes, Lidar).

2.4 FTIR ozone time series

Figure 2 displays the time series of ozone total columns at each ground-based FTIR station. Because we consider only solar absorption measurements, the time series at Ny-Alesund, Thule, and Kiruna cover only the Mid-March–September, Late-February–Mid-October and Mid-January–Mid-November periods, respectively. The seasonal variation is isolated in Fig. 3 which shows the monthly mean total columns over the periods of measurements. We clearly see

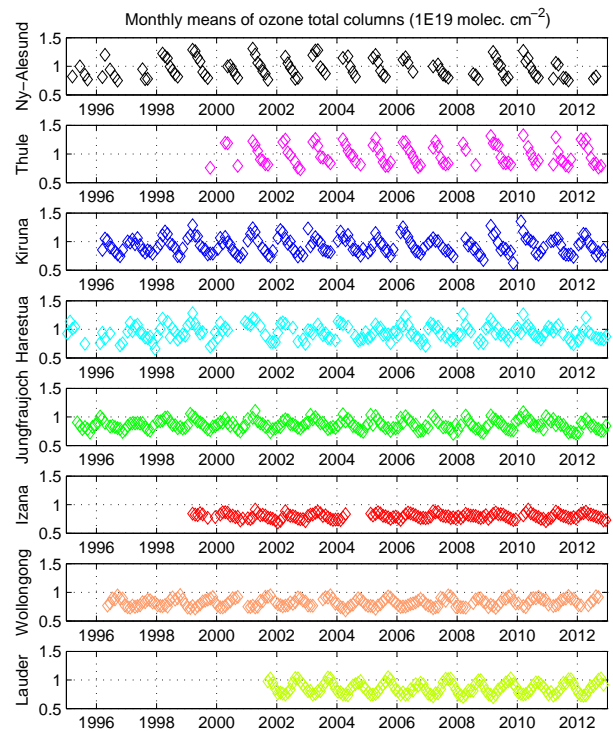


Fig. 2. Time series of monthly means of ozone total columns at each station.

the well-known seasonal cycle of ozone total column having a maximum in spring at all stations, and the higher amplitude of the seasonal variation at higher latitudes (Brosseur and Solomon, 1984).

Figure 3 shows also the monthly means of the four partial columns defined in the previous section (Table 3). In the upper stratospheric layer, the ozone maximum occurs in summer (early summer at high latitudes shifting to late

summer with decreasing latitude), in agreement with higher photo-chemical production of ozone during this season. In the lower stratospheric layer, the ozone maximum is in late winter/early spring at all latitudes. The situation is more **variable** for the middle stratospheric layer: still late winter/early spring for Harestua, Jungfraujoch, Lauder and Wollongong, but the latter shows a second maximum in late summer, and a small amplitude of the seasonal cycle. For the three higher latitude stations Ny-Alesund, Thule and Kiruna, the maximum is still in spring, extending to May for the two latter stations. At Izaña, the maximum is in summer in the middle stratosphere. For the tropospheric column, we observe a maximum in spring at all stations, but at Jungfraujoch it extends also in summer.

3 Multiple regression model

The ozone FTIR total and partial column trends in Vigouroux et al. (2008); WMO (2010); García et al. (2012) were calculated with a bootstrap re-sampling method, applied to the daily means time series. In these studies, only the seasonal cycle and a linear trend were taken into account, the remaining natural ozone variability was then an additional noise in the ozone trend determination. To reduce the uncertainties on the trends and to better understand what drives ozone variability and trends, we use in the present study a multiple linear regression (MLR) model. To reduce the auto-correlation in the residuals, we use here the monthly means time series. **Furthermore, to account for the still significant auto-correlation in the residuals, a Cochran-Orcutt transformation (Cochran and Orcutt, 1949) is applied to the final model. This gives more reliable confidence intervals for the regression parameters.**

The following regression model is applied to the monthly means of ozone total and partial column time series $Y(t)$:

$$Y(t) = A_0 + A_1 \cdot \cos(2\pi t/12) + A_2 \cdot \sin(2\pi t/12) + A_3 \cdot \cos(4\pi t/12) + A_4 \cdot \sin(4\pi t/12) + A_5 \cdot t + \sum_{k=6}^n A_k \cdot X_k(t) + \epsilon(t), \quad (2)$$

where **A_0 is the intercept**, the A_1 to A_4 parameters describe the ozone seasonal cycle, A_5 is the annual trend, $X_k(t)$ are the explanatory variables (proxies time series) and A_k their respective coefficient, and $\epsilon(t)$ represents the residuals.

To select the final regression model, we have included several proxies, which represent processes that are known to impact ozone, in a stepwise regression procedure that keeps or rejects each proxy: the initial model (seasonal cycle and trend) is fitted first. Second, iteratively, if any proxies, not already in the model, have p values less than an entrance tolerance (0.05) i.e. if it is unlikely that they would have zero coefficient if added to the model, then we add the one with the smallest p value. Otherwise, if any proxies in the model have

p values greater than an exit tolerance (0.10), then we remove the one with the largest p value and we repeat the whole process until no single step improves the model. Hence, the final set of parameters can vary with the station and with the partial columns concerned. In this paper, a proxy is called “non-significant” when it has not been retained by the stepwise procedure. This choice of not using a fixed model for all stations and partial columns avoids to over-fit the data, and is justified by the large latitudinal range of the stations (e.g., the VPSC or ENSO proxies will not impact the stations in the same way), and by the different processes driving ozone variability at different altitudes.

The proxies that have been tested in the stepwise regression procedure are summarized in Table 4. The two most common explanatory variables found in the literature are the solar radio flux at F10.7 cm (SOLAR) which represents the 11 year solar cycle (following e.g. Newchurch et al., 2003; Randel and Wu, 2007), and the zonal winds measured at Singapore at 30 and 10 hPa (following e.g. Brunner et al., 2006) which represent the quasi-biennial oscillation (QBO). The proxy used for the El Niño-Southern Oscillation (ENSO) is the Multivariate ENSO Index (MEI), following Randel et al. (2009). Different time-lags (from 0 to 4 months) between ENSO and ozone time series have been tested. The other dynamical proxies that have been explored are the tropopause pressure (TP) at each station (following e.g. Appenzeller et al., 2000), the equivalent latitude (EL) at three altitude levels around each station, the Arctic Oscillation (AO) or the Antarctic Oscillation (AAO) indices depending on the station location (e.g. Appenzeller et al., 2000; Frossard et al., 2013), and the vertical component of the Eliassen-Palm flux (EPF) at 100 hPa averaged over 45 to 75° north and south, as a proxy for the Brewer-Dobson circulation (e.g. Brunner et al., 2006). **These dynamical proxies are connected, e.g. the NAO (North Atlantic Oscillation, closely related to AO) and the tropopause pressure (Appenzeller et al., 2000), the eddy heat flux (proportional to EPF) and the AO (Weber et al., 2011), but we let the stepwise regression model choose the most adapted proxy for each station and partial column.** Concerning the equivalent latitude, we did not construct an integrated equivalent proxy valuable for the whole ozone “integrated” total column as in Wohltmann et al. (2005). Here, we simply use the equivalent latitude calculated from ERA Interim reanalysis (Dee et al., 2011) at three altitude levels corresponding approximately to the middle of our three stratospheric layers (ELL for LowS, ELM for MidS, and ELU for UppS; see Table 3 for the layer limits), namely at 370, 550, and 950 K, respectively, for all stations except Izaña and Wollongong (460, 700, and 1040 K, respectively). Lastly, the volume of polar stratospheric clouds (VPSC) is used as a proxy for polar ozone loss (e.g. Brunner et al., 2006). The VPSC proxy has been multiplied by the effective equivalent stratospheric chlorine (EESC) time series calculated with a mean age of air of 5.5 years, in order to take into account the time for the ozone depleting substances to

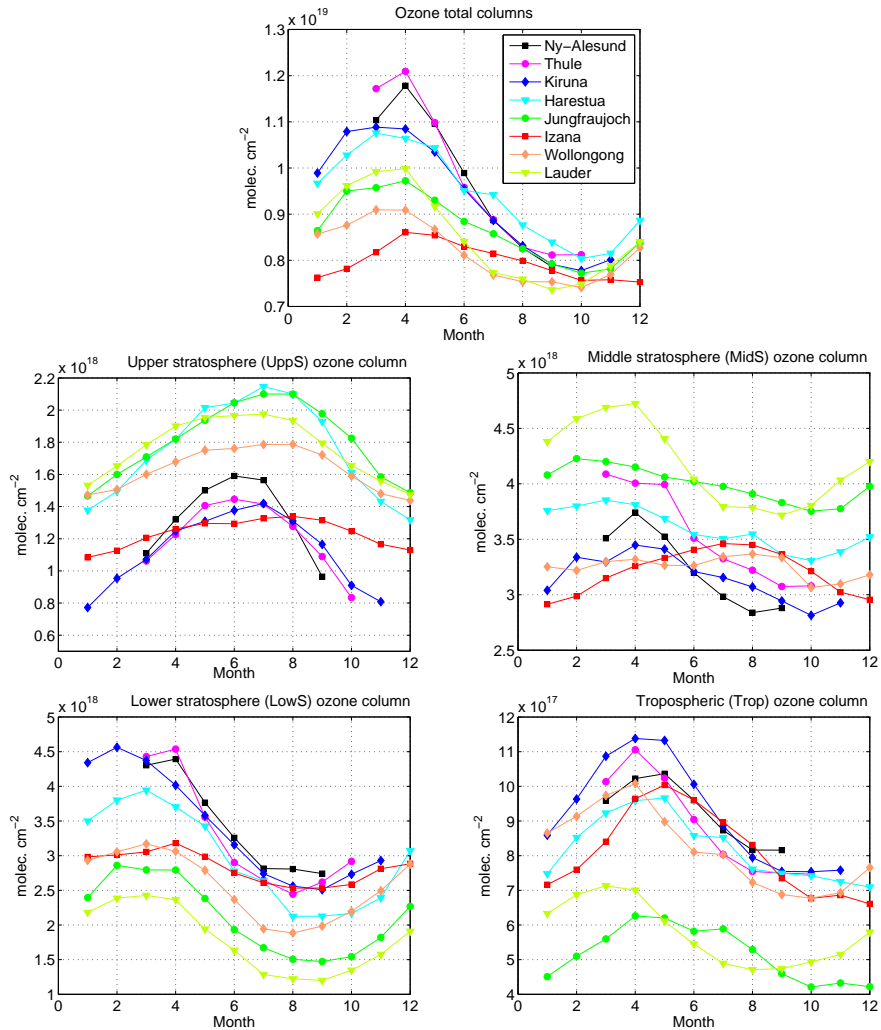


Fig. 3. Monthly means of ozone total and partial columns for the whole periods of measurements. See Table 3 for the limits of the partial columns at each station. The seasonal cycle for Southern Hemisphere stations, Wollongong and Lauder, has been shifted by 6 months for better comparison.

reach the poles (http://acdb-ext.gsfc.nasa.gov/Data_services/automailler/index.html). To account for the cumulative effect over months of the EPF and the VPSC*EESC proxies on ozone, we have followed the approach of Brunner et al. (2006) (see their Eq. 4), **with the same dependence of their constant τ on season and latitude of the station.**

For the two QBO proxies (30 and 10 hPa), if retained in the stepwise procedure, four seasonal parameters can be added to the model. The $A_k \cdot X_k(t)$ term of Eq. (2) is then replaced by:

$$(A_k + A_{k+1} \cdot \cos(2\pi t/12) + A_{k+2} \cdot \sin(2\pi t/12) + A_{k+3} \cdot \cos(4\pi t/12) + A_{k+4} \cdot \sin(4\pi t/12)) \cdot X_k(t). \quad (3)$$

Depending on the station and on the layer, none, one or both of the two proxies QBO30 and QBO10 will be retained in the model, with or without their additional seasonal parameters.

We will call from here “QBO contribution”, the sum of all possible contributions of QBO30 and QBO10.

Since the time series involved in the present study start at earliest in 1995, we do not include two commonly used explanatory variables: the aerosol optical thickness needed to represent the effect on ozone of the large volcanic eruptions of El Chichón (1982) and Mount Pinatubo (1991), and the EESC proxy which can be used as direct proxy for the halogen loading of the stratosphere instead of the piecewise linear trend (PWLT) with a turnaround in 1996/1997 often used in time series starting well before this turnaround point (WMO, 2010). Our linear trend estimates are therefore better comparable to the studies which use the PWLT method. At polar stations, the turnaround is occurring a few years later, so that the use of the EESC proxy could be an alternative to the simple linear trend for these stations. However, we preferred to

Table 4. Name, short description, and source of the proxies that have been tested in the stepwise regression model.

Name	Description	Source
SOLAR	Solar Radio Flux at 10.7 cm	ftp://ftp.ngdc.noaa.gov/STP/SOLAR_DATA/SOLAR_RADIO/FLUX/Penticton_Adjusted/monthly/MONTHLY.ADJ
QBO30	zonal winds measured at Singapore at 30 hPa	http://www.geo.fu-berlin.de/en/met/ag/strat/produkte/qbo/index.html
QBO10	zonal winds measured at Singapore at 10 hPa	http://www.geo.fu-berlin.de/en/met/ag/strat/produkte/qbo/index.html
ENSO	Multivariate ENSO Index (MEI)	http://www.esrl.noaa.gov/psd/enso/mei/
AO/AO	Arctic Oscillation	http://www.cpc.ncep.noaa.gov/products/precip/CWlink/daily_ao_index/monthly.ao.index.b50.current.ascii
	Antarctic Oscillation	http://www.cpc.ncep.noaa.gov/products/precip/CWlink/daily_ao_index/aao/monthly.aao.index.b79.current.ascii
TP	Tropopause pressure	http://www.esrl.noaa.gov/psd/data/gridded/data.ncep.reanalysis.tropopause.html
EL(L/M/U)	Equivalent latitude at three altitude levels: 370, 550, and 950 K: high/mid-latitude stations 460, 700, and 1040 K: subtropical stations	calculated at BIRA from ERA interim reanalysis
EPF	Vertical component of the EP flux	http://www.awi.de/en/research/research_divisions/climate_science/atmospheric_circulations/projects/candidoz/ep_flux_data/
VPSC	Volume of Polar Stratospheric Clouds	calculated at FMI

adopt the same approach for all the stations. Probably, when the FTIR record will be longer, one would be able to distinguish between the EESC impact on ozone and a possible additional trend due to process(es) that are not represented in the model.

4 Results and discussion

In Fig. 4, we show the individual contribution C_{frac} of each proxy retained by the stepwise procedure to the coefficient of determination $R^2 = \sum C_{\text{frac}}$, for each station and partial column. The individual contribution C_{frac} of a proxy is the product of the standardized regression coefficient of this proxy with the correlation coefficient between the proxy and the observations (Scherrer, 1984). In Fig. 4, the seasonal parameters contribution (A_1 to A_4 in Eq. 2), which gives in most cases the very dominant part of the explained variability, is not shown for better clarity of the other proxies contribution. But we give it for completeness in Table 5, together with R^2 . In the following discussion, we will highlight some selected features which are visible in the ozone time series and which can be attributed to a specific proxy. The final MLR model is the sum of all the significant proxies, and therefore the effect of a specific proxy can be visible in the plots in some years, but masked in other years.

In Table 6, we give the annual ozone trend at each station for each layer obtained with the stepwise multiple linear regression model. The uncertainties on the trends correspond to the 95 % percent confidence interval. A trend is considered significant if it is larger than the uncertainty.

4.1 High latitude stations

In addition to the three Arctic stations Ny-Alesund, Thule and Kiruna, we will consider Harestua (60° N) as a high latitude station since, in terms of trends, Harestua appears to behave similarly to the Arctic stations.

4.1.1 Tropospheric (Trop) columns

In the troposphere, the high latitude stations, except Kiruna, show negative significant ozone trends (Table 6). The spatial and temporal variability in the Arctic and the different sampling at the stations Thule/Ny-Alesund due to polar night (see Fig. 2) makes it difficult to compare the trend results. We see in Fig. 5 that at Ny-Alesund the negative trend occurs in the second part of the period (2004–2012), which is also observed at Thule (not shown). On the contrary, at Harestua, the negative trend is occurring in the 1999–2007 period (Fig. 5, lower left panel). The second line of Fig. 5 shows the partial columns where the seasonal cycle is removed for emphasizing the interannual variability, and the effect of individual proxies showing interannual differences. We have added in the third line of Fig. 5 the VPSC signal, i.e. the VPSC proxy time series multiplied by the corresponding parameter obtained in the MLR process ($A_k \cdot X_k(t)$ in Eq. 2). We see that the particular low tropospheric values in 1995, 2005 and 2011 at Ny-Alesund can be related to the VPSC proxy, therefore by the influence of lower stratospheric ozone variability on the tropospheric columns. At the three other stations, this VPSC impact was not found to be significant, and the main driver of tropospheric variability is found to be the tropopause pressure TP (Fig. 4). The larger VPSC value in 1996 does not lead to a larger decrease in tropospheric ozone because it is compensated by a positive QBO signal, while

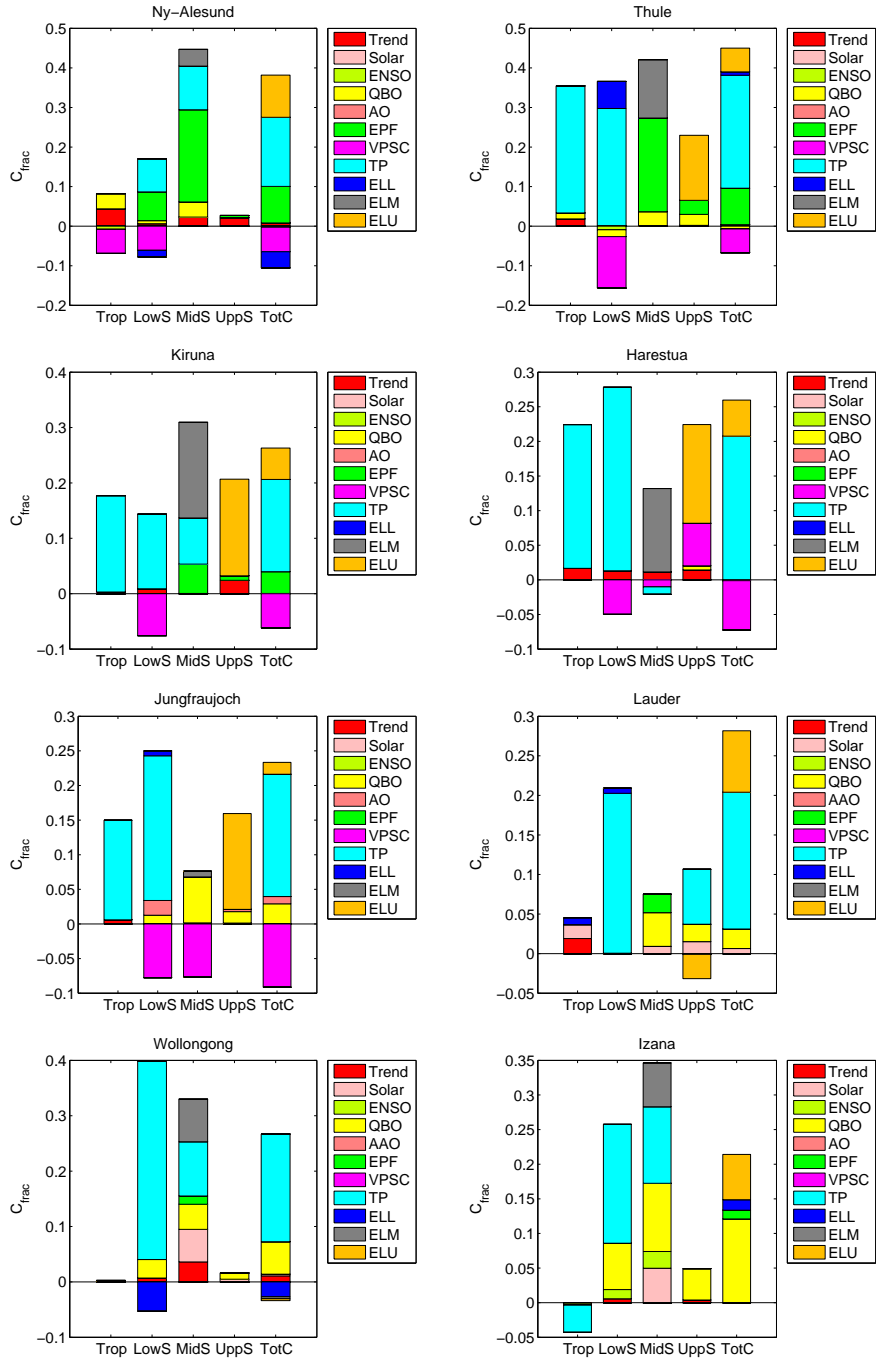


Fig. 4. Individual contributions C_{frac} of the proxies to the coefficient of determination R^2 . R^2 and the dominant contribution of the seasonal cycle C_{seas} are given in Table 5.

Table 5. Coefficient of determination R^2 and contribution of the seasonal cycle C_{seas} determined within the final model. See Table 3 for the limits of the layers, different for subtropical stations and mid/high latitude stations.

FTIR station	Trop	LowS	MidS	UppS	Total columns
Ny-Alesund	$R^2 = 0.75$ $C_{\text{seas}} = 0.73$	$R^2 = 0.92$ $C_{\text{seas}} = 0.82$	$R^2 = 0.72$ $C_{\text{seas}} = 0.27$	$R^2 = 0.74$ $C_{\text{seas}} = 0.72$	$R^2 = 0.95$ $C_{\text{seas}} = 0.68$
Thule	$R^2 = 0.86$ $C_{\text{seas}} = 0.50$	$R^2 = 0.92$ $C_{\text{seas}} = 0.71$	$R^2 = 0.83$ $C_{\text{seas}} = 0.41$	$R^2 = 0.81$ $C_{\text{seas}} = 0.58$	$R^2 = 0.96$ $C_{\text{seas}} = 0.58$
Kiruna	$R^2 = 0.85$ $C_{\text{seas}} = 0.67$	$R^2 = 0.89$ $C_{\text{seas}} = 0.82$	$R^2 = 0.54$ $C_{\text{seas}} = 0.23$	$R^2 = 0.78$ $C_{\text{seas}} = 0.58$	$R^2 = 0.89$ $C_{\text{seas}} = 0.69$
Harestua	$R^2 = 0.77$ $C_{\text{seas}} = 0.54$	$R^2 = 0.74$ $C_{\text{seas}} = 0.51$	$R^2 = 0.36$ $C_{\text{seas}} = 0.25$	$R^2 = 0.67$ $C_{\text{seas}} = 0.45$	$R^2 = 0.75$ $C_{\text{seas}} = 0.56$
Jungfraujoch	$R^2 = 0.73$ $C_{\text{seas}} = 0.58$	$R^2 = 0.83$ $C_{\text{seas}} = 0.66$	$R^2 = 0.53$ $C_{\text{seas}} = 0.53$	$R^2 = 0.93$ $C_{\text{seas}} = 0.77$	$R^2 = 0.81$ $C_{\text{seas}} = 0.67$
Izaña	$R^2 = 0.83$ $C_{\text{seas}} = 0.87$	$R^2 = 0.72$ $C_{\text{seas}} = 0.46$	$R^2 = 0.80$ $C_{\text{seas}} = 0.45$	$R^2 = 0.69$ $C_{\text{seas}} = 0.64$	$R^2 = 0.77$ $C_{\text{seas}} = 0.56$
Wollongong	$R^2 = 0.69$ $C_{\text{seas}} = 0.69$	$R^2 = 0.86$ $C_{\text{seas}} = 0.52$	$R^2 = 0.42$ $C_{\text{seas}} = 0.09$	$R^2 = 0.77$ $C_{\text{seas}} = 0.75$	$R^2 = 0.87$ $C_{\text{seas}} = 0.63$
Lauder	$R^2 = 0.89$ $C_{\text{seas}} = 0.85$	$R^2 = 0.94$ $C_{\text{seas}} = 0.73$	$R^2 = 0.78$ $C_{\text{seas}} = 0.70$	$R^2 = 0.89$ $C_{\text{seas}} = 0.82$	$R^2 = 0.95$ $C_{\text{seas}} = 0.66$

Table 6. Annual trend (in % decade⁻¹) and their 95 % uncertainty ranges. Due to polar night, the measurements at Ny-Alesund, Thule and Kiruna cover only the Mid-March–September, Late-February–Mid-October, and Mid-January–Mid-November periods, respectively. All time series end in September/December 2012 for the present study. The time of start is repeated for each station. See Table 3 for the limits of the layers, different for subtropical stations and mid/high latitude stations. Trends indicated in bold are significant.

FTIR station	Trop	LowS	MidS	UppS	Total columns
Ny-Alesund	-5.8 ± 3.2	-4.2 ± 3.1	-5.5 ± 3.8	+6.7 ± 5.3	-3.0 ± 1.5
1995					
Thule	-5.3 ± 4.4	-0.4 ± 6.3	+0.2 ± 4.4	-2.3 ± 6.5	-2.1 ± 2.6
1999 (October)					
Kiruna	-0.9 ± 2.5	-3.9 ± 2.6	+0.4 ± 2.6	+7.4 ± 3.4	-0.3 ± 1.6
1996					
Harestua	-3.1 ± 2.0	-5.3 ± 4.6	+4.8 ± 4.3	+7.8 ± 5.5	+1.0 ± 2.2
1995					
Jungfraujoch	-2.5 ± 2.7	-0.5 ± 3.3	-0.6 ± 1.2	+0.9 ± 1.0	-0.4 ± 1.2
1995					
Izaña	+0.7 ± 2.8	-1.7 ± 2.2	-0.1 ± 2.0	+1.6 ± 2.6	+0.5 ± 1.2
1999					
Wollongong	-2.2 ± 2.8	+3.1 ± 2.7	+4.0 ± 2.0	+0.2 ± 1.6	+1.9 ± 1.1
1996					
Lauder with /	+7.7 ± 3.5	-3.8 ± 4.1	-0.2 ± 3.5	+2.8 ± 2.4	-0.3 ± 1.8
without SOLAR	+5.0 ± 4.4	-	-1.1 ± 3.4	+1.7 ± 2.4	-0.6 ± 1.9
2001					

the small ozone value in 2004 is related to a negative QBO signal (not shown).

As expected, the large VPSC values in 1995, 2005 and 2011 have also a significant impact on the lower stratospheric

(LowS) values at Ny-Alesund (middle column of Fig. 5), as well as in 1996, since the negative effect is not compensated by QBO signal as in Trop. We can note that the VPSC impact is ten times larger in LowS than in Trop (different scales in Fig. 5).

4.1.2 Lower stratospheric (LowS) columns

The VPSC proxy is found significant at the four high latitude stations for the lower stratospheric columns, being the main driver of ozone variability after TP (Fig. 4). We give the example of Ny-Alesund and Kiruna in Fig. 5, where the effect of large amount of VPSC in 1996, 2005, and 2011 is clearly visible in both monthly means and deseasonalized time series. We show in addition the EPF and TP signals at Ny-Alesund and Kiruna, respectively, in the bottom panel. It can be seen that the TP signal at Kiruna in 2005 also contributed to even lower ozone that particular year. The larger LowS values at Ny-Alesund in 1999 is due to a combination of the TP (not shown) and EPF signals.

In the lower stratosphere, at all high latitude stations, except Thule, we observe significant negative trends (Table 6). At Thule, the shorter time period associated with the high variability of this layer at high latitude gives a large uncertainty on the trend.

4.1.3 Middle stratospheric (MidS) columns

The results are mixed for the middle stratospheric layers, as noticed previously for the seasonal cycles. The trend is significantly negative at Ny-Alesund and non-significant at Thule. The trend is non-significant at Kiruna, and significantly positive at Harestua. The EPF proxy explains about 25 % of the variability at Ny-Alesund and Thule, and about 5 % at Kiruna (Fig. 4). This is illustrated in Fig. 6 for Ny-Alesund and Thule, where we see nicely the same features at both stations in the middle stratospheric columns (e.g. higher columns in 2009, 2010; lower columns in 2011), associated with the EPF time series.

4.1.4 Upper stratospheric (UppS) columns

In the upper stratosphere, the three stations with similar time periods show a significant positive trend. In the three cases, the increase in ozone partial columns occurs in the 1995–2003 period, after which a leveling off is observed (Fig. 7). If we run the MLR model on the same time period as Thule (October 1999–2012), all the stations show non-significant trends. Since the EESCs were still increasing until about 2000 at polar regions (WMO, 2010), the significant positive trends obtained at high latitude stations in the upper stratosphere cannot be explained by the effect of Montréal Protocol on ozone depleting substances. At present we do not have an explanation for this increase in ozone during the 1995–2003 period. The 11 year solar cycle might contribute to it, since the increase in solar activity from 1996 to its maximum in

2001–2002 is in phase with the ozone increase during the same period. The solar cycle signal at Ny-Alesund shown in Fig. 7 as an illustration turns out to be non-significant after the Cochrane-Orcutt transformation is applied, so its contribution is small and not visible in Fig. 4. The solar cycle might be found non-significant at the other stations because the expected decrease of ozone during the declining phase of the solar cycle (2002–2009) is not observed. This could be a sign that this decrease is compensated by a positive linear trend, which could be due to the declining EESCs, but also to the increase of greenhouse gases (WMO, 2010). More years are needed to understand unequivocally the increase in 1995–2003, followed by a leveling off, and distinguish between the ozone responses due to solar cycle, EESCs and possible proxies not included in the present study.

4.1.5 Total columns

We observe that the total column ozone trends are small and non-significant at all high latitude stations, except at Ny-Alesund ($-3.0 \pm 1.5 \%$ decade⁻¹ or -10.8 ± 5.6 DU decade⁻¹). The negative trend at Ny-Alesund occurs in the 2003–2012 period, as for the lowest altitude layers. At all stations, the dominant contributions to the total column variability are the TP, the VPSC, the ELU, and, except at Harestua, the EPF proxies. We see nicely in Table 5, how well the proxies explained the additional variability at the Arctic stations, e.g. at Ny-Alesund $R^2 = 0.95$, compared to the contribution of the seasonal cycle $C_{\text{seas}} = 0.68$.

4.2 Mid-latitude and subtropical stations

We have two mid-latitude stations in this study (Jungfraujoch, 47° N and Lauder, 45° S), and two subtropical stations (Izaña, 28° N and Wollongong, 34° S).

4.2.1 Tropospheric (Trop) columns

The tropospheric trends are non-significant at Jungfraujoch, Izaña and Wollongong, and significantly positive at Lauder. The trend at Jungfraujoch is $-2.5 \pm 2.7 \%$ decade⁻¹, but we see in Fig. 8 that the tropospheric columns are increasing up to 1999 and then show a linear decrease, in agreement with aircraft and surface alpine sites in the study of Logan et al. (2012). If we limit our time period to the 1998–2008 period as in Logan et al. (2012), we also find a significant negative trend ($-6.3 \pm 4.9 \%$ decade⁻¹). But this is largely due to the high ozone values 1998–1999, and for the period 2000–2012 we obtain still a non-significant trend of $-2.9 \pm 3.4 \%$ decade⁻¹. At Izaña, the tropospheric trends derived from ozonesondes were found non-significant in García et al. (2012), in agreement with our study, but the uncertainties were large. The situation is more mixed in the Southern Hemisphere: the tropospheric trend at Wollongong is not significant while it is significantly positive at

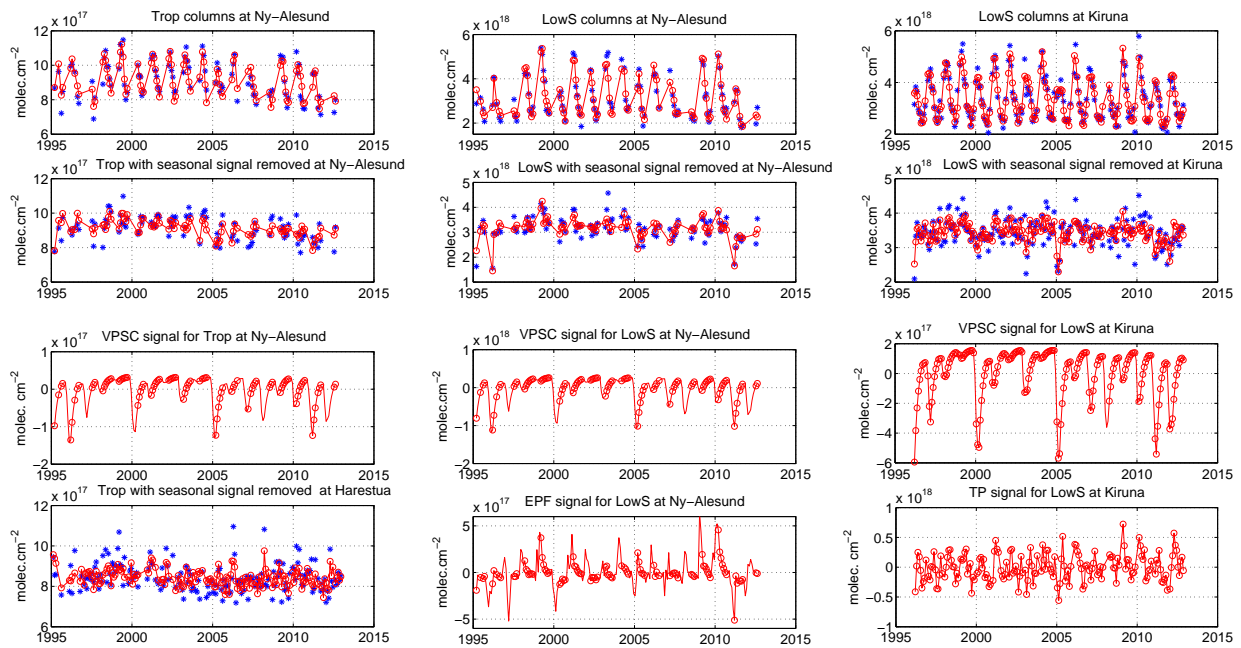


Fig. 5. Left (top to bottom panels): 1) monthly means of the tropospheric columns (Trop) at Ny-Alesund (blue: FTIR, red: MLR model); 2) same but with the seasonal signal removed; 3) the VPSC signal obtained from the MLR model for Trop at Ny-Alesund, for each month of the period (red line), and at each FTIR observed month (red circle); 4) monthly means of Trop at Harestua with the seasonal cycle removed. Middle panels: 1-3) same as left panels but for the lower stratospheric columns (LowS) at Ny-Alesund; 4) the EPF signal obtained for the LowS at Ny-Alesund. Right panels: 1-3) same as middle panels but at Kiruna; 4) the tropopause pressure (TP) signal obtained for the LowS at Kiruna.

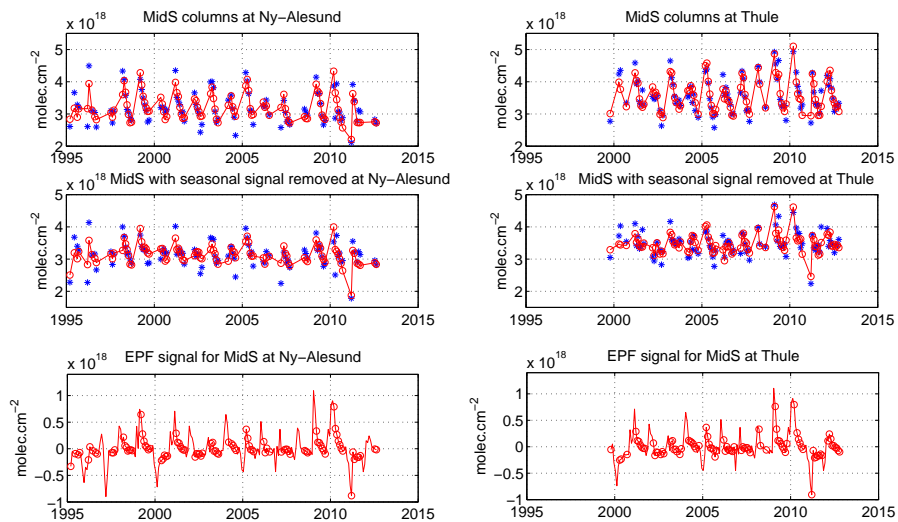


Fig. 6. Top panels: monthly means of the middle stratospheric columns (MidS) at Ny-Alesund (left) and Thule (right) (blue: FTIR, red: MLR model). Middle panels: same but with the seasonal signal removed. Bottom panels: the EPF signal obtained in each case from the MLR model, for each month of the period (red line), and at each FTIR observed month (red circle).

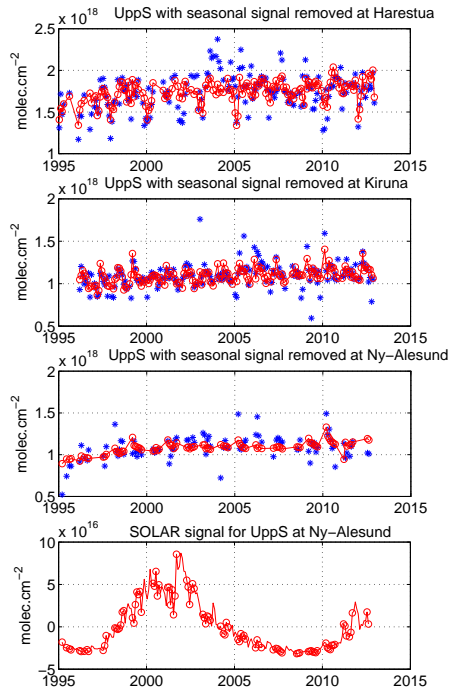


Fig. 7. Monthly means of the upper stratospheric columns (UppS) with the seasonal cycle removed, from top to bottom: Harestua, Kiruna and Ny-Alesund (blue: FTIR, red: MLR model). Bottom panel: the solar cycle signal obtained at Ny-Alesund from the MLR model, before the Cochrane-Orcutt transformation.

Lauder ($+7.7 \pm 3.5 \%$ decade $^{-1}$). The trend at Lauder is in agreement with the study of Oltmans et al. (2013) who obtain about $+5 \%$ decade $^{-1}$ in the lower and middle troposphere with ozonesondes measurements at Lauder. We find a significant positive impact of the solar cycle at Lauder and it is clearly seen in Fig. 8. This is not in agreement with Chandra et al. (1999), in which the solar cycle shows a strong but negative impact on tropospheric columns for non-polluted region. At Lauder at present only a short time period (2001–2012) is available for trend studies, and we hope to have more clarification on this subject with more years of data. However, if we remove the solar cycle proxy from the MLR model, we still obtain a significant trend of $+5.0 \pm 4.4 \%$ decade $^{-1}$. **For this short time-series, we have added in Table 6 the trends that are obtained if the solar cycle is removed from the model.**

4.2.2 Lower stratospheric (LowS) columns

The trends in the lower stratosphere are non-significant at Jungfraujoch, Izaña and Lauder, and significantly positive at Wollongong. The cause of the significant positive trend at Wollongong is not fully explained at present. A part of it is due to a small negative trend in the ELL proxy. If we remove this proxy from the MLR model, we observe a non-

significant positive trend of $+2.4 \pm 2.8 \%$ decade $^{-1}$.

The dominant proxy is TP for all stations. At the Jungfraujoch station, the VPSC proxy, which in the case of Jungfraujoch corresponds to the transport of polar ozone loss to mid-latitudes, explains about 8 % of the variability (Fig. 4). The VPSC proxy is non-significant at the southern hemispheric station Lauder, in agreement with more stable and isolated vortex in the Antarctic compared to the Arctic. The Arctic Oscillation (AO) proxy is found significant at Jungfraujoch while the corresponding AAO proxy is non-significant at Lauder.

We show the time series of the lower stratospheric columns at Jungfraujoch in Fig. 9 together with the AO and QBO signals. We see that in 2010 ozone shows larger values, and that this is explained by the combination of a very negative AO index (the corresponding parameter in the MLR is negative and gives the positive signal in 2010 shown in Fig. 9) and easterly phase of the QBO. This is in agreement with Nair et al. (2013), who applied a MLR model to the mean of ozone anomalies at Observatoire de Haute-Provence (OHP) from different instruments (Lidar, ozonesondes and satellites). However, we did not find a significant contribution from the EPF proxy, which according to Nair et al. (2013) also contributed to the high ozone values in 2010. We can state that our vertical and total column ozone trends are in agreement with the Nair et al. (2013) results when taking the error bars into account, but the latter study found significant positive trends at OHP while our trends at Jungfraujoch are all non-significant.

As expected, the QBO contribution to ozone variability is more important at the subtropical station Izaña, which is also the only station where the ENSO proxy was found to make a significant, but small, contribution to the variability (Fig. 4). We illustrate the QBO effect at Izaña in Fig. 9, for total columns.

4.2.3 Middle stratospheric (MidS) columns

The situation for the middle stratosphere is very similar to that of the lower stratosphere: all trends are found non-significant except at Wollongong where it is positive. It is in this 23–32 km layer for subtropical stations that the solar cycle shows the most important contribution (Fig. 4). This is not what has been reported in Randel and Wu (2007) and Tourpali et al. (2007), where the ozone response to solar cycle was maximum in the tropical lower and upper stratosphere, and minimum in the middle stratosphere. At Wollongong, the middle stratospheric ozone response is about 6 % between solar minimum and solar maximum (see Fig. 9) while values of 1 % have been reported (Sioris et al., 2014) at about 25 km. However, the recent work of Chiodo et al. (2014) shows that the apparent solar cycle signal in the tropical lower stratosphere for the period 1960–2004 is due to the two volcanic eruptions El Chichón in 1982 and Mt. Pinatubo in 1991, and the authors find robust solar cycle signals only

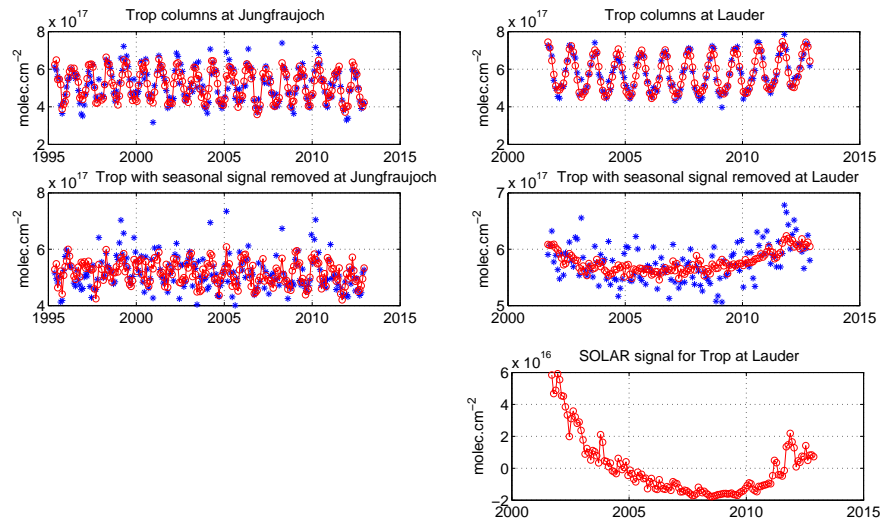


Fig. 8. Top panels: monthly means of the tropospheric columns (Trop) at Jungfraujoch (left) and Lauder (right) (blue: FTIR, red: MLR model). Middle panels: same but with the seasonal signal removed. Bottom panel: the solar cycle signal obtained at Lauder from the MLR model.

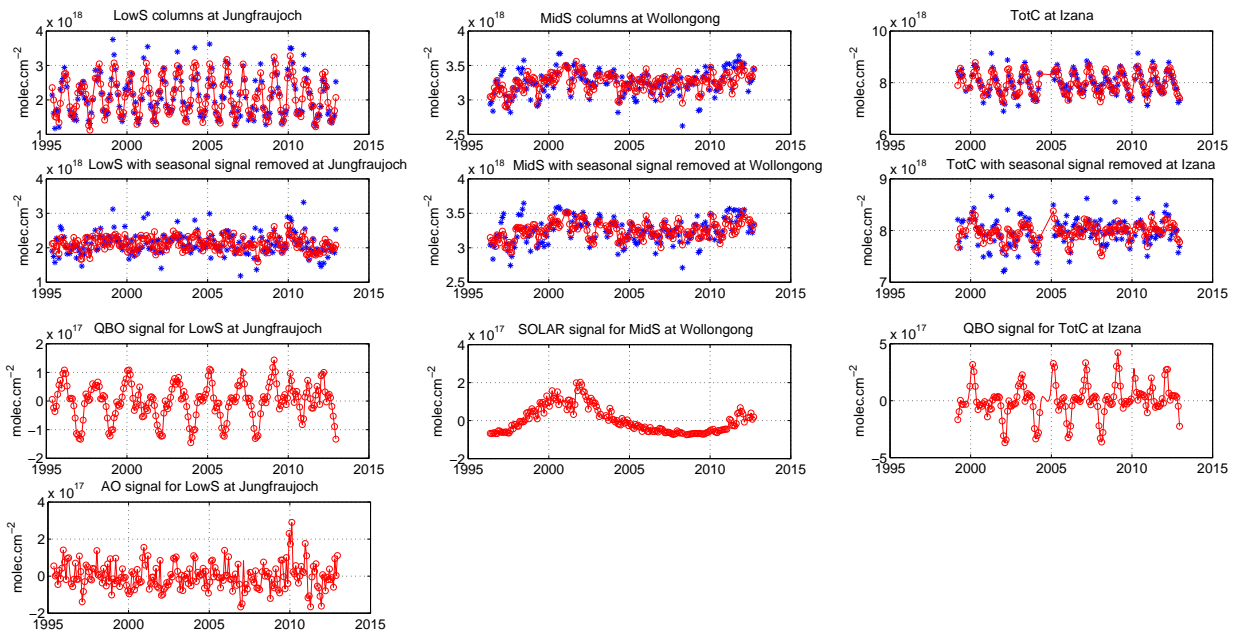


Fig. 9. Top panels: monthly means of the lower stratospheric columns (LowS) at Jungfraujoch (left), middle stratospheric columns (MidS) at Wollongong (middle), and total columns (TotC) at Izaña (middle) (right). (blue: FTIR, red: MLR model). Middle panels: same but with the seasonal signal removed. Bottom panels: QBO and AO signals obtained from the MLR model at Jungfraujoch (left), SOLAR signal at Wollongong (middle), and QBO signal at Izaña (right).

in the middle and upper stratosphere. In the upper stratospheric layer at Wollongong, the response to the solar cycle is indeed also significant and is about 2.5% between solar minimum and solar maximum which is in agreement with previous studies (WMO, 2010). At Izaña, the solar contribution is found negative in the 23–32 km layer, which seems doubtful. Again, this concerned one of the shortest time series of the study (1999–2012), and could be corrected with future measurements.

4.2.4 Upper stratospheric (UppS) columns

The trends in the upper stratospheric layer are all positive in these latitudes, but significant only at Lauder ($+2.8 \pm 2.4\%$ decade⁻¹). Our trend at Jungfraujoch station ($+0.9 \pm 1.0\%$ decade⁻¹) corresponds well to the observed trend ($+1.5\%$ decade⁻¹) at OHP in Nair et al. (2013) in the 31–39 km range, although it is found significant in this latter study. The MLR model explains 93% of the variability at Jungfraujoch ($R^2 = 0.93$), namely 77% of the variability comes from the seasonality and the remaining 16% from the proxies, mainly the ELU and QBO (see Fig. 4). At Lauder, the trend in the 30–40 km range from Lidar measurements is also found significantly positive for the period 2000–2012 with trend values ($+2\text{--}3\%$ decade⁻¹) similar to FTIR (W. Steinbrecht, personal communication, 2013). If we remove the solar cycle signal in the MLR for the short time-series of Lauder, the trend becomes smaller and non-significant ($+1.7 \pm 2.4\%$ decade⁻¹). More years of data will improve the confidence in the solar cycle signal in the short time-series.

4.2.5 Total columns

The total column trends are non-significant at the mid-latitude stations ($-0.4 \pm 1.2\%$ decade⁻¹ or -1.4 ± 3.8 DU decade⁻¹ at Jungfraujoch, $-0.3 \pm 1.8\%$ decade⁻¹ or -1.1 ± 5.9 DU decade⁻¹ at Lauder), non-significant at Izaña ($+0.5 \pm 1.2\%$ decade⁻¹ or $+1.4 \pm 3.6$ DU decade⁻¹), and significantly positive at Wollongong ($+1.9 \pm 1.1\%$ decade⁻¹ or $+5.8 \pm 3.5$ DU decade⁻¹). The total column trend at Jungfraujoch is in agreement within error bars with the result of Nair et al. (2013) at OHP when they use the PWLT method ($+5.5 \pm 3.3$ DU decade⁻¹), but again the trend at OHP is found significantly positive. When the EESC proxy is used in their study a trend of $+4.2 \pm 0.8$ DU decade⁻¹ is found. The same behaviour is seen more globally in a recent study using merged satellite data from 1979 to 2012 (Chehade et al., 2014): for the latitude of Jungfraujoch, the trends are about $+3\text{--}4$ DU decade⁻¹ for the 1997–2012 period, and non-significant if the PWLT method is used, while significant when the EESC proxy is used, which decreases the uncertainty on the trends. It seems that at Jungfraujoch, our time series is still too short to observe this

positive trend. At the latitude of Izaña, the merged satellite data set shows a $+3\text{--}4$ DU decade⁻¹ for the 1997–2012 period, with the more recent SBUV/SBUV-2 MOD v8.6, non-significant using the PWLT (in agreement with our study) and significant using the EESC proxy. Since our time series start at best in 1995, the EESC proxy is not really “separable” from a linear trend study at our mid-latitude and subtropical stations. When more years of data will become available, the same sensitivity study (PWLT vs EESC) could be tested at least for polar stations where the turnaround point is expected around 2000.

It is also interesting to note that, using the PWLT method, at the latitude of Wollongong, Chehade et al. (2014) found a positive significant trend of about $+3$ DU decade⁻¹, while at the latitude of Lauder the trend is decreased to about $+1$ DU decade⁻¹ (non-significant) in good agreement with what FTIR observed. When they use the EESC proxy, the trend is increasing with latitude, so that at the Lauder latitude, it reaches about $4\text{--}5$ DU decade⁻¹.

Our non-significant trends at Jungfraujoch, Izaña and Lauder, and positive trend at Wollongong are also in agreement with the recent study of Coldevey-Egbers et al. (2014), which provides trends using a similar period (1995–2013) of merged satellite data sets. For Wollongong, since the total column positive trend is due to the ozone trends in the lower and middle stratosphere, it cannot be attributed unambiguously to the EESCs decline.

5 Conclusions

We have exploited the time series of ozone total and partial columns (Trop, LowS, MidS, UppS) at 8 NDACC FTIR stations (Ny-Alesund, 79° N; Thule, 77° N; Kiruna, 68° N; Harestua, 60° N; Jungfraujoch, 47° N; Izaña, 28° N; Wollongong, 34° S; Lauder, 45° S) to derive vertically resolved trends, using a MLR model including the main proxies well-known for impacting the ozone variability.

After the seasonal variation, the TP proxy is the dominant driver of ozone variability at all stations, mainly for the troposphere, lower stratosphere and total columns, while the EL proxy is an important contributor to the middle and upper stratosphere, as well as to the total column variabilities. At the highest latitude stations (68 to 79° N), the EPF proxy contributes substantially to the middle stratospheric and total column variabilities. The VPSC proxy for polar ozone loss contributes to the lower stratosphere and total columns variabilities at the Arctic stations, but also at Jungfraujoch while it is non-significant at the southern hemispheric station Lauder. At the mid-latitude and subtropical stations, the QBO proxy is a substantial contributor to ozone variability, especially at the lowest latitude station, Izaña. The AO/AO and ENSO proxies are significant only at Jungfraujoch and Izaña, respectively. At Wollongong, the 2.5% ozone response to solar cycle in the upper layer is in agree-

ment with previous studies, but the response in the middle stratosphere ($\sim 6\%$) is much larger than previously reported ($\sim 1\%$). The 11 year solar cycle effect is still subject of debate (WMO, 2010; Chiodo et al., 2014), so that an additional decade of measurements would help in fixing its real impact on ozone. This is particularly true for our shortest time series, Lauder, Izaña and Thule.

The trends at the high latitude stations are negative in the troposphere, except at Kiruna where it is non-significant. Except at Thule, the high latitude stations show significant negative trends in the lower stratosphere. The situation is mixed in the middle stratosphere, where the trend is significantly negative at Ny-Alesund, non-significant at Thule and Kiruna, and significantly positive at Harestua. The trends of the three high latitude stations with a similar time-period are all positive in the upper stratosphere, but this increase is taking place during the 1995–2003 period, while the EESC were still increasing until about 2000 in the polar region (WMO, 2010). However all four stations give non-significant trends in the upper stratosphere for the October 1999–2012 period, which could be the onset of the upper stratospheric ozone recovery at high latitude. The total column trends are non-significant at all high latitude stations, except at Ny-Alesund where it is negative. This is in agreement (except at Ny-Alesund) with model predictions that the Arctic March ozone recovery to 1980 levels will occur around 2026 (WMO, 2010). However, the high year-to-year total column variability at these latitudes, driven mainly by lower stratospheric variability due to the polar temperature variations, does not allow yet to draw conclusions from the current trends for Arctic total ozone in the coming few years.

The trends for mid-latitude and subtropical stations are all non-significant, except at Lauder in the troposphere and upper stratosphere, and at Wollongong for the total columns and the lower and middle stratospheric columns. Some signs of the onset of ozone mid-latitude recovery are observed only in the Southern Hemisphere, while a few more years seems to be needed to observe it at the northern stations.

To conclude, among the numerous available satellite and ground-based data sets measuring vertical distributions of ozone that are useful for ozone trend evaluations (Hassler et al., 2014), the NDACC ground-based FTIR measurements have their particular assets. **Indeed, several stations, well distributed around the globe, are now reaching almost 20 years of measurements and will continue measuring ozone in the future: to the eight stations of this work could be added, after homogenization of the retrieval analysis and/or few more years of data, Eureka (80°N), Rikubetsu (44°N), Bremen (53°N), Mauna Loa (20°N), Arrival Heights (78°S). This provides long time series of ozone that are reliable over time, provided that the ILS is properly taken into account.** This is also the only data set, with Umkehr measurements, that provides simultaneously total columns, tropospheric columns and three stratospheric columns that reach 40–45 km. This data set is suitable for an alternative determination of ozone

vertical changes, as **demonstrated** in this study, but also for validation of the satellite merged data sets and detection of possible drifts.

Acknowledgements. The National Center for Atmospheric Research is supported by the National Science Foundation. The observation program at Thule, Greenland, is supported under contract by the National Aeronautics and Space Administration and the site is also supported by the NSF Office of Polar Programs. We wish to thank the Danish Meteorological Institute for support at the Thule. We would like to thank U. Raffalski and P. Völger for technical support at IRF Kiruna. The University of Liège team acknowledges the support of the F.R.S. – FNRS, the Fédération Wallonie-Bruxelles, the International Foundation High Altitude Research Stations Jungfrauoch and Gornergrat (HFSJG, Bern) and Meteoswiss. The NIWA Lauder MIR-FTIR project is core funded through New Zealand’s Ministry of Business, Innovation and Employment. We are grateful to the many colleagues having contributed to FTIR data acquisition at the various sites. We wish to thank S. Godin-Beekmann and M. Pastel (LATMOS) for useful discussion on equivalent latitude proxy, and R. Kivi (KMI) for discussion on ozonesondes trends in the Arctic. This study has been supported by the EU FP7 project NORS, the ESA PRODEX project A3C, as well as the AGACC-II project within the “Science for a Sustainable Development” research program funded by the Belgian Science Policy Office.

References

- Appenzeller, C., Weiss, A. K., and Staehelin, J.: North Atlantic Oscillation modulates total ozone winter trends, *Geophys. Res. Lett.*, 27, 1131–1134, 2000.
- Barret, B., De Mazière, M., and Demoulin, P.: Retrieval and characterization of ozone profiles from solar infrared spectra at the Jungfrauoch, *J. Geophys. Res.*, 107, 4788, doi:10.1029/2001JD001298, 2002.
- Bodeker, G. E., Hassler, B., Young, P. J., and Portmann, R. W.: A vertically resolved, global, gap-free ozone database for assessing or constraining global climate model simulations, *Earth Syst. Sci. Data*, 5, 31–43, doi:10.5194/essd-5-31-2013, 2013.
- Brasseur, G. and Solomon, S: *Aeronomy of the Middle Atmosphere*, 441 pp., D. Reidel Publishing Company, Dordrecht, Holland, 1984.
- Brunner, D., Staehelin, J., Maeder, J. A., Wohltmann, I., and Bodeker, G. E.: Variability and trends in total and vertically resolved stratospheric ozone based on the CATO ozone data set, *Atmos. Chem. Phys.*, 6, 4985–5008, doi:10.5194/acp-6-4985-2006, 2006.
- Chandra, S., Ziemke, J. R., and Stewart, R. W.: An 11-year solar cycle in tropospheric ozone from TOMS measurements, *Geophys. Res. Lett.*, 26, 185–188, 1999.
- Chehade, W., Weber, M., and Burrows, J. P.: Total ozone trends and variability during 1979–2012 from merged data sets of various satellites, *Atmos. Chem. Phys.*, 14, 7059–7074, doi:10.5194/acp-14-7059-2014, 2014.
- Chiodo, G., Marsh, D. R., Garcia-Herrera, R., Calvo, N., and García, J. A.: On the detection of the solar signal in the tropical stratosphere, *Atmos. Chem. Phys.*, 14, 5251–5269, doi:10.5194/acp-14-5251-2014, 2014.

- Cochrane, D. and Orcutt, G. H.: Application of least squares regression to relationships containing auto-correlated error terms, *J. Am. Stat. Assoc.*, 44, 32–61, 1949.
- Coldewey-Egbers, M., Loyola, D. G., Braesicke, P., Dameris, M., van Roozendaal, M., Lerot, C., and Zimmer, W.: A new health check of the ozone layer at global and regional scales, *Geophys. Res. Lett.*, 41, 4363–4372, doi:10.1002/2014GL060212, 2014.
- Dee, D. P., Uppala, S. M., Simmons, A. J., Berrisford, P., Poli, P., Kobayashi, S., Andrae, U., Balmaseda, M. A., Balsamo, G., Bauer, P., Bechtold, P., Beljaars, A. C. M., van de Berg, L., Bidlot, J., Bormann, N., Delsol, C., Dragani, R., Fuentes, M., Geer, A. J., Haimberger, L., Healy, S. B., Hersbach, H., Hólm, E. V., Isaksen, I., Kållberg, P., Köhler, M., Matricardi, M., McNally, A. P., Monge-Sanz, B. M., Morcrette, J.-J., Park, B.-K., Peubey, C., de Rosnay, P., Tavolato, C., Thépaut, J.-N., and Vitart, F.: The ERA-Interim reanalysis: configuration and performance of the data assimilation system, *Q. J. Roy. Meteor. Soc.*, 137, 553–597, doi:10.1002/qj.828, 2011.
- Frossard, L., Rieder, H. E., Ribatet, M., Staehelin, J., Maeder, J. A., Di Rocco, S., Davison, A. C., and Peter, T.: On the relationship between total ozone and atmospheric dynamics and chemistry at mid-latitudes – Part 1: Statistical models and spatial fingerprints of atmospheric dynamics and chemistry, *Atmos. Chem. Phys.*, 13, 147–164, doi:10.5194/acp-13-147-2013, 2013.
- García, O. E., Schneider, M., Redondas, A., González, Y., Hase, F., Blumenstock, T., and Sepúlveda, E.: Investigating the long-term evolution of subtropical ozone profiles applying ground-based FTIR spectrometry, *Atmos. Meas. Tech.*, 5, 2917–2931, doi:10.5194/amt-5-2917-2012, 2012.
- Garcia, R. R., Marsh, D. R., Kinnison, D. E., Boville, B. A., and Sassi, F.: Simulation of secular trends in the middle atmosphere, 1950–2003, *J. Geophys. Res.*, 112, D09301, doi:10.1029/2006JD007485, 2007.
- Hase, F., Blumenstock, T., and Paton-Walsh, C.: Analysis of the instrumental line shape of high-resolution Fourier transform IR spectrometers with gas cell measurements and new retrieval software, *Appl. Optics*, 38, 3417–3422, 1999.
- Hase, F.: Inversion von Spurengasprofilen aus hochaufgelösten bodengebundenen FTIR-Messungen in Absorption, Dissertation, Wissenschaftliche Berichte Forschungszentrum Karlsruhe, FZKA 6512; ISSN 0947–8620, Forschungszentrum Karlsruhe, Karlsruhe, Germany, 2000.
- Hase, F., Hannigan, J. W., Coffey, M. T., Goldman, A., Höpfner, M., Jones, N. B., Rinsland, C. P., and Wood, S. W.: Intercomparison of retrieval codes used for the analysis of high-resolution, ground-based FTIR measurements, *J. Quant. Spectrosc. Ra.*, 87, 25–52, 2004.
- Hassler, B., Petropavlovskikh, I., Staehelin, J., August, T., Bharatia, P. K., Clerbaux, C., Degenstein, D., Mazière, M. De, Dinelli, B. M., Dudhia, A., Dufour, G., Frith, S. M., Froidevaux, L., Godin-Beekmann, S., Granville, J., Harris, N. R. P., Hoppel, K., Hubert, D., Kasai, Y., Kurylo, M. J., Kyrölä, E., Lambert, J.-C., Levelt, P. F., McElroy, C. T., McPeters, R. D., Munro, R., Nakajima, H., Parrish, A., Raspollini, P., Remsberg, E. E., Rosenlof, K. H., Rozanov, A., Sano, T., Sasano, Y., Shiotani, M., Smit, H. G. J., Stiller, G., Tamminen, J., Tarasick, D. W., Urban, J., van der A, R. J., Veefkind, J. P., Vigouroux, C., von Clarmann, T., von Savigny, C., Walker, K. A., Weber, M., Wild, J., and Zawodny, J. M.: Past changes in the vertical distribution of ozone – Part 1: Measurement techniques, uncertainties and availability, *Atmos. Meas. Tech.*, 7, 1395–1427, doi:10.5194/amt-7-1395-2014, 2014.
- Kyrölä, E., Laine, M., Sofieva, V., Tamminen, J., Päivärinta, S.-M., Tukiainen, S., Zawodny, J., and Thomason, L.: Combined SAGE II–GOMOS ozone profile data set for 1984–2011 and trend analysis of the vertical distribution of ozone, *Atmos. Chem. Phys.*, 13, 10645–10658, doi:10.5194/acp-13-10645-2013, 2013.
- Logan, J. A., Staehelin, J., Megretskaja, I. A., Cammas, J.-P., Thouret, V., Claude, H., De Backer, H., Steinbacher, M., Scheel, H.-E., Stübi, R., Fröhlich, M., and Derwent, R.: Changes in ozone over Europe: Analysis of ozone measurements from sondes, regular aircraft (MOZAIC) and alpine surface sites, *J. Geophys. Res.*, 117, D09301, doi:10.1029/2011JD016952, 2012.
- Mikuteit, S.: Trendbestimmung stratosphärischer Spurengase mit Hilfe bodengebundener FTIR-Messungen, Dissertation, Forschungszentrum Karlsruhe, FZK Report No. 7385, Germany, 2008.
- Nair, P. J., Godin-Beekmann, S., Kuttippurath, J., Ancellet, G., Goutail, F., Pazmiño, A., Froidevaux, L., Zawodny, J. M., Evans, R. D., Wang, H. J., Anderson, J., and Pastel, M.: Ozone trends derived from the total column and vertical profiles at a northern mid-latitude station, *Atmos. Chem. Phys.*, 13, 10373–10384, doi:10.5194/acp-13-10373-2013, 2013.
- Newchurch, M. J., Yang, E.-S., Cunnold, D. M., Reinsel, G. C., Zawodny, J. M., and Russell III, J. M.: Evidence for slowdown in stratospheric ozone loss: First stage of ozone recovery, *J. Geophys. Res.*, 108, 4507, doi:10.1029/2003JD003471, 2003.
- Oltmans, S. J., Lefohn, A. S., Shadwick, D., Harris, J. M., Scheel, H. E., Galbally, I., Tarasick, D. W., Johnson, B. J., Brunke, E.-G., Claude, H., Zeng, G., Nichol, S., Schmidlin, F., Davies, J., Cuevas, E., Redondas, A., Naoe, H., Nakano, T., Kawasato, T.: Recent tropospheric ozone changes – a pattern dominated by slow or no growth, *Atmos. Environ.*, 67, 331–351, 2013.
- Pougatchev, N. S., Connor, B. J., and Rinsland, C. P.: Infrared measurements of the ozone vertical distribution above Kitt Peak, *J. Geophys. Res.*, 100, 16689–16697, 1995.
- Randel, W. J., and Wu, F.: A stratospheric ozone profile data set for 1979–2005: Variability, trends, and comparisons with column ozone data, *J. Geophys. Res.*, 112, D06313, doi:10.1029/2006JD007339, 2007.
- Randel, W. J., Garcia, R. R., Calvo, N., and Marsh, D.: ENSO influence on zonal mean temperature and ozone in the tropical lower stratosphere, *Geophys. Res. Lett.*, 36, L15822, doi:10.1029/2009GL039343, 2009.
- Rodgers, C. D.: Inverse methods for atmospheric sounding: Theory and Practice, Series on Atmospheric, Oceanic and Planetary Physics – Vol. 2, World Scientific Publishing Co., Singapore, 2000.
- Rothman, L. S., Gordon, I. E., Barbe, A., Benner, D. C., Bernath, P. F., Birk, M., Boudon, V., Brown, L. R., Campargue, A., Champion, J.-P., Chance, K., Coudert, L. H., Danaj, V., Devi, V. M., Fally, S., Flaud, J.-M., Gamache, R. R., Goldman, A., Jacquemart, D., Kleiner, I., Lacome, N., Lafferty, W. J., Mandin, J.-Y., Massie, S. T., Mikhailenko, S. N., Miller, C. E., Moazzen-Ahmadi, N., Naumenko, O. V., Nikitin, A. V., Orphal, J., Perevalov, V. I., Perrin, A., Predoi-Cross, A., Rinsland, C. P., Rotger, M., Šimečková, M.,

- Smith, M. A. H., Sung, K., Tashkun, S. A., Tennyson, J., Toth, R. A., Vandaele, A. C., and Vander Auwera, J.: The Hitran 2008 molecular spectroscopic database, *J. Quant. Spectrosc. Ra.*, 110, 533–572, 2009.
- Scherrer, B.: Biostatistique, Gaëtan Morin, Chicoutimi, 1984.
- Schneider, M., Hase, F., and Blumenstock, T.: Ground-based remote sensing of HDO/H₂O ratio profiles: introduction and validation of an innovative retrieval approach, *Atmos. Chem. Phys.*, 6, 4705–4722, doi:10.5194/acp-6-4705-2006, 2006.
- Sioris, C. E., McLinden, C. A., Fioletov, V. E., Adams, C., Zawodny, J. M., Bourassa, A. E., Roth, C. Z., and Degenstein, D. A.: Trend and variability in ozone in the tropical lower stratosphere over 2.5 solar cycles observed by SAGE II and OSIRIS, *Atmos. Chem. Phys.*, 14, 3479–3496, doi:10.5194/acp-14-3479-2014, 2014.
- Sussmann, R., Borsdorff, T., Rettinger, M., Camy-Peyret, C., Demoulin, P., Duchatelet, P., Mahieu, E., and Servais, C.: Technical Note: Harmonized retrieval of column-integrated atmospheric water vapor from the FTIR network – first examples for long-term records and station trends, *Atmos. Chem. Phys.*, 9, 8987–8999, doi:10.5194/acp-9-8987-2009, 2009.
- Tikhonov, A.: On the solution of incorrectly stated problems and a method of regularization, *Dokl. Acad. Nauk SSSR*, 151, 501–504, 1963.
- Tourpali, K., Zerefos, C. S., Balis, D. S., and Bais, A. F.: The 11-year solar cycle in stratospheric ozone: comparison between Umkehr and SBUVv8 and effects on surface erythema irradiance, *J. Geophys. Res.*, 112, D12306, doi:10.1029/2006JD007760, 2007.
- Vigouroux, C., De Mazière, M., Demoulin, P., Servais, C., Hase, F., Blumenstock, T., Kramer, I., Schneider, M., Mellqvist, J., Strandberg, A., Velasco, V., Notholt, J., Sussmann, R., Stremme, W., Rockmann, A., Gardiner, T., Coleman, M., and Woods, P.: Evaluation of tropospheric and stratospheric ozone trends over Western Europe from ground-based FTIR network observations, *Atmos. Chem. Phys.*, 8, 6865–6886, 2008.
- Weber, M., Dikty, S., Burrows, J. P., Garny, H., Dameris, M., Kubin, A., Abalichin, J., and Langematz, U.: The Brewer-Dobson circulation and total ozone from seasonal to decadal time scales, *Atmos. Chem. Phys.*, 11, 11221–11235, doi:10.5194/acp-11-11221-2011, 2011.
- World Meteorological Organization: Atmospheric Ozone: 1985, Global Ozone Research and Monitoring Project – Report No. 16, Geneva, 1998.
- World Meteorological Organization: Scientific Assessment of Ozone Depletion: 1998, Global Ozone Research and Monitoring Project – Report No. 44, Geneva, 1998.
- World Meteorological Organization: Scientific Assessment of Ozone Depletion: 2010, Global Ozone Research and Monitoring Project – Report No. 52, Geneva, 2011.
- Wohlmann, I., Rex, M., Brunner, D., and Mäder: Integrated equivalent latitude as a proxy for dynamical changes in ozone column, *Geophys. Res. Lett.*, 32, L09811, doi:10.1029/2005GL022497, 2005.